

Characterizing the Speciation, Distribution, and Correlation of Heavy Metals in Mine Wastes Using Synchrotron Radiation Techniques

Final Technical Report for MRERP Award # 06HQGR0181

Christopher S. Kim

Department of Chemistry, Program in Environmental Sciences
Chapman University
One University Drive
Orange, CA 92867

Research supported by the U.S. Geological Survey (USGS), Department of the Interior, under USGS award number 06HQGR0181. The views and conclusions contained in this document are those of the authors and should not be interpreted as necessarily representing the official policies, either expressed or implied, of the U.S. Government.

Comparison of Accomplishments with Established Goals

The two primary goals and related hypotheses associated with each goal are presented herein verbatim from the awarded proposal, followed by a general discussion of the work accomplished and its relation to the specific goal.

Goal 1: Using bulk EXAFS spectroscopy, quantitatively characterize speciation trends of Hg and As in mine wastes from different Hg deposit types (silica-carbonate, epithermal hot-spring) as a function of 1) particle size and 2) distance from the mine site.

Hypothesis: The total concentrations of Hg and As will increase as particle size and distance from the host mine decrease, while the proportions of less soluble Hg and As phases will decrease with particle size and distance due to preferential weathering and dissolution of more soluble phases. Hg-chloride phases will be more prevalent among the hot-spring Hg deposits due to elevated chloride concentrations during their formation.

Due to the development of new strategic goals from the USGS and BLM, focus was shifted from Hg mines in the CA Coast Range to the Kelly and Randsburg mining districts in the high desert region of Southern-Central California. These mines were primarily explored for Au and Ag and have associated concentrations of arsenic ranging as high as >10,000 ppm total As. Thus, concentration, distribution, and speciation trends were largely focused on As levels rather than Hg for the duration of this grant period. Nevertheless, the general trends and associations studied were still in keeping with the grant's primary goals. Extensive sampling was conducted throughout the Randsburg mining district, including samples collected of tailings piles, waste rock, soil profiles, and distributed sediment deposits.

Following manual size separation of selected samples using stainless steel sieves to generate 11 discrete size fractions, trends in concentration of heavy metals as a function of particle size were assessed through the development of an Excel spreadsheet template that auto-generates graphs for the concentrations of 48 elements analyzed by ICP-MS. These were combined with the mass distribution of the sample to similarly auto-generate graphs of elemental mass distribution for each of the 48 elements. An example of this process is given in Figure 1, showing as a function of particle size (decreasing from S1 to S11 as described in the initial proposal) the mass distribution of the sample (Figure 1a), the concentration trend of arsenic (Figure 1b), and the mass distribution of arsenic in the samples (Figure 1c).

As shown in Figure 1, the concentration trend for arsenic demonstrates an inverse relationship between particle size and concentration as initially hypothesized; such a trend has been observed for arsenic in the majority of samples and suggests that relatively insoluble and soft As-bearing phases are becoming preferentially concentrated in the fine-grained size fractions. Other trends have been observed and categorized for all elements analyzed for individual samples; a schematic of the different trends observed is shown in Figure 2. This allows the grouping of elements that share similar concentration trends for further analysis using microspectroscopic methods. A list of all samples that have undergone such size separation and analysis is provided in Appendix A.

We have begun bulk analysis using extended X-ray absorption fine structure (EXAFS) spectroscopy to determine the speciation of arsenic in selected samples. This is accomplished by comparing the EXAFS spectrum collected from the sample to a spectral library of well-characterized As species through a linear combination fitting method that identifies both the phases present and their relative proportions to one another. Examples of this fitting method as applied to mine tailings from the Randsburg and Kelly mining districts are shown in Figures 3 and 4, respectively. Compiled results from EXAFS speciation analysis of multiple samples are shown in Figure 5, indicating that the As phase scorodite ($\text{FeAsO}_4 \cdot 2\text{H}_2\text{O}$) is present in the Kelly samples but not in the Randsburg samples, while arseniosiderite ($\text{Ca}_2\text{Fe}_3(\text{AsO}_4)_3\text{O}_2 \cdot 3\text{H}_2\text{O}$) and arsenic sorbed to iron oxyhydroxide phases are generally dominant throughout both mine sites.

Goal 2: Apply microspectroscopic methods to low-concentration (<100 ppm) mine wastes, utilizing micro-X-ray fluorescence (uXRF), micro-EXAFS (uEXAFS), and micro-X-ray diffraction (uXRD) techniques to assess the speciation, distribution, and correlation of metals associated with the ore metals in samples that could not otherwise be analyzed by bulk EXAFS spectroscopy.

Hypothesis: Speciation of Hg and As in low-concentration samples will reveal an enrichment in relatively insoluble phases due to their persistence at low levels. Hg is expected to be concentrated as discrete mineralized particles while As may be more widely distributed among individual grains and sorbed species associated with Fe-oxides. The distribution of other significant metals including Co, Cd, Cr, Cu, Ni, Pb, and Zn will be assessed by these techniques to determine whether they are present as discrete metal-rich grains or dispersed as sorbed or amorphous phases.

Considerable progress has been made on exploring the capabilities of microspectroscopic methods for the analysis of mine waste samples, particularly as a function of particle size. Due to either the absence of necessary instrumentation or the low time investment/quality ratio for data collection, uXRD and uEXAFS were largely eschewed in favor of focusing on uXRF analysis. Still, a wealth of data was generated which provide intriguing insights into the distribution and relationships of metals with one another.

Selected size fractions from samples chosen based on results from the previously-described bulk concentration analyses were investigated using uXRF methods, resulting in finely-detailed (i.e. resolution as small as 2x2 um) spatial maps that could selectively express the relative intensities of over a dozen different elements. A list of samples and size fractions analyzed using microspectroscopic methods is provided in Appendix B. For simplicity's sake this report will describe our findings regarding the observed relationship between As and Fe, which was initially observed in the bulk concentration analyses as discussed earlier.

Comparing the As and Fe elemental distribution maps side-by-side, it becomes apparent that the two elements are generally associated with one another, and furthermore that particles containing both elements appear to fall within one of two categories: those with a relatively high As:Fe ratio and those with a relatively low As:Fe ratio (Figure 6). This can be expressed more readily by generating a correlation plot (Figure 7) that plots the relative fluorescence counts for As and

Fe for every pixel in the map, showing clearly the two populations of particles noted in the elemental distribution maps.

In a number of selected samples a similar association between As and Fe has been observed; this is both consistent with the bulk concentration data and the bulk EXAFS speciation analysis described earlier and shows excellent agreement between the different analytical methods in determining the speciation of arsenic in the mine tailings samples investigated. An additional observation seen among several samples has been an increase in the number of populations (represented as pixels forming lines or “fingers” of constant slope in the correlation plots) with decreasing particle size. This may represent an increasing diversity of As-bearing phases in the finer size fractions and/or the sorption of As to different iron oxide phases resulting in different As:Fe ratios. Ongoing work on these associations and those of other pairs of metals is continuing from the data collected thus far.

Work Products Produced

In addition to this performance report, a manuscript is in preparation entitled “Particle-Size Dependence on Metal Concentrations in Mine Wastes” (authors Kim, C.S., Wilson, K., and Rytuba, J.J.) focusing on the bulk concentration analyses which will be submitted to Environmental Science & Technology by the end of this calendar year. Shortly thereafter we anticipate submitting a second manuscript presenting our findings using bulk and microscale spectroscopic methods by February 2008.

Research funded by the MRERP was presented at the following professional conferences, with students’ names provided in bold:

Kim, C.S. and Rytuba, J.J. “Trends in metal speciation and distribution within mine wastes as a function of particle size.” Oral presentation at 2007 Geological Society of America Annual Meeting, October 2007, Denver, CO.

Miller S.R., Sugihara E., Petersen N., Mortera H., and Kim C.S. “Leach testing of mine wastes: environmental impact and metal mobility in water supplies and body fluids.” Poster presentation at 2007 Geological Society of America Annual Meeting, October 2007, Denver, CO.

Wilson, K.M., Rytuba, J.J., and Kim, C.S. “Trends In metal concentrations and associations as a function Of particle size In mine wastes.” Poster presentation at 2007 Geological Society of America Annual Meeting, October 2007, Denver, CO.

Kim, C.S. and Rytuba, J.J. “Characterizing the speciation, distribution, and correlations of heavy metals in mine wastes.” Invited oral presentation at 2007 SSRL/LCLS Users Meeting, October 2007, Stanford, CA.

Miller, S., Wilson, K., Sugihara, E. and Kim, C.S. “Speciation of metal-bearing mine wastes using micro X-ray fluorescence.” Poster presentation at 2007 SSRL/LCLS Users Meeting, October 2007, Stanford, CA.

Kim, C.S. and Rytuba, J.J. "Particle size effects on heavy metal distribution, speciation, and correlations in mine wastes." Invited oral presentation at 17th V.M. Goldschmidt geochemistry conference, August 2007, Cologne, Germany.

Finally, this project has resulted in the creation of a detailed and sophisticated template for the autogeneration of mass distribution, elemental concentration, and elemental mass distribution trends as a function of particle size that will continue to be used for future sample characterization. An example of one such template is provided in Appendix C.

Concluding Remarks

The insights gained from the research funded by the MRERP have considerably advanced our understanding of trends in concentration, speciation, distribution, and correlations between metals in mine wastes as a function of particle size and will inform or have informed current and future investigations by the grant recipient and his research group. The techniques developed and applied as part of this project will continue to be of use in ongoing characterizations of additional mine sites as part of a formal collaboration between the recipient, the USGS, and the BLM.

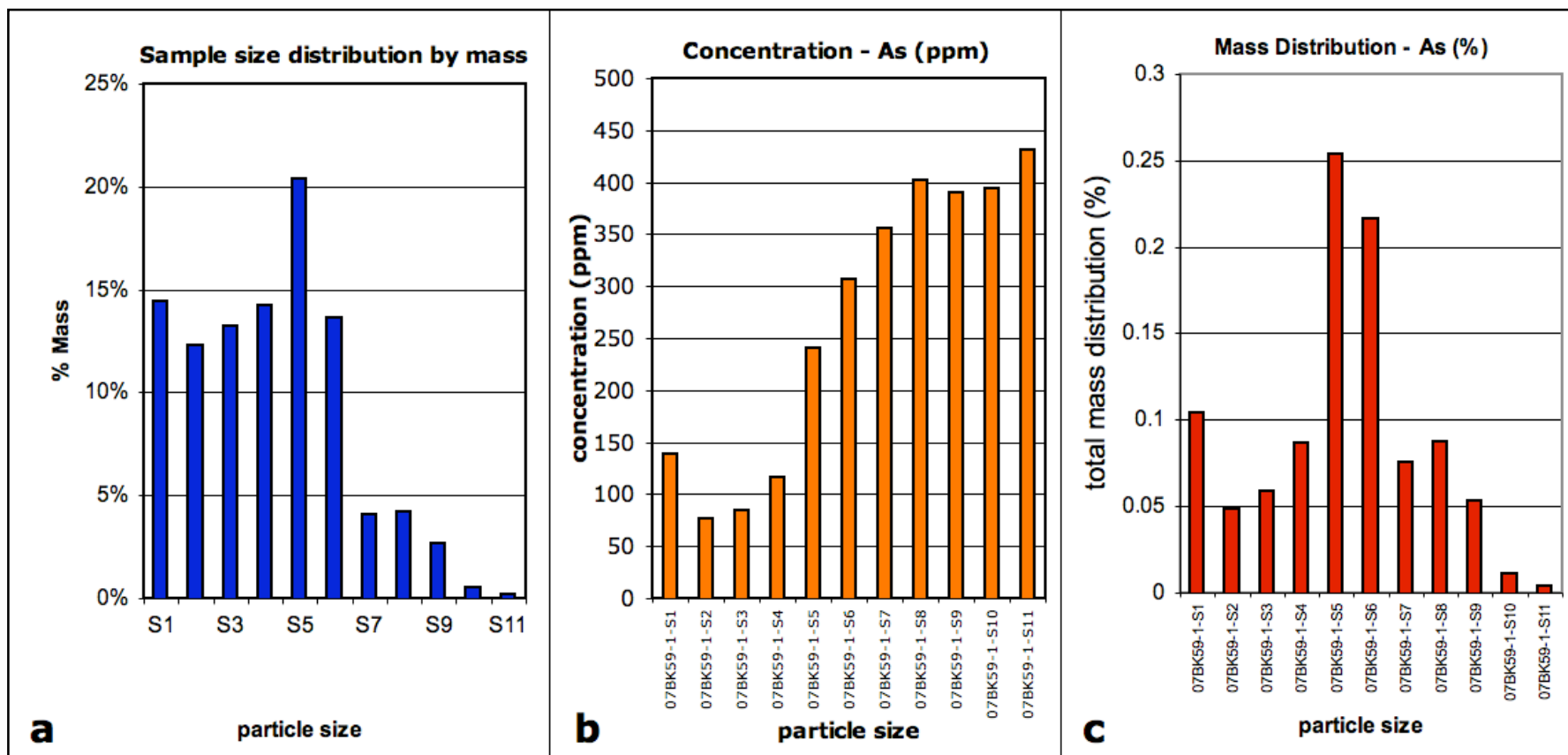


Figure 1. Example of bulk mass and concentration trend data generated for each size-separated sample. (a) Sample mass distribution as a function of particle size. (b) Concentration of each element (arsenic shown only) as a function of particle size. (c) Mass distribution of each element (arsenic shown only) within the sample as a function of particle size.

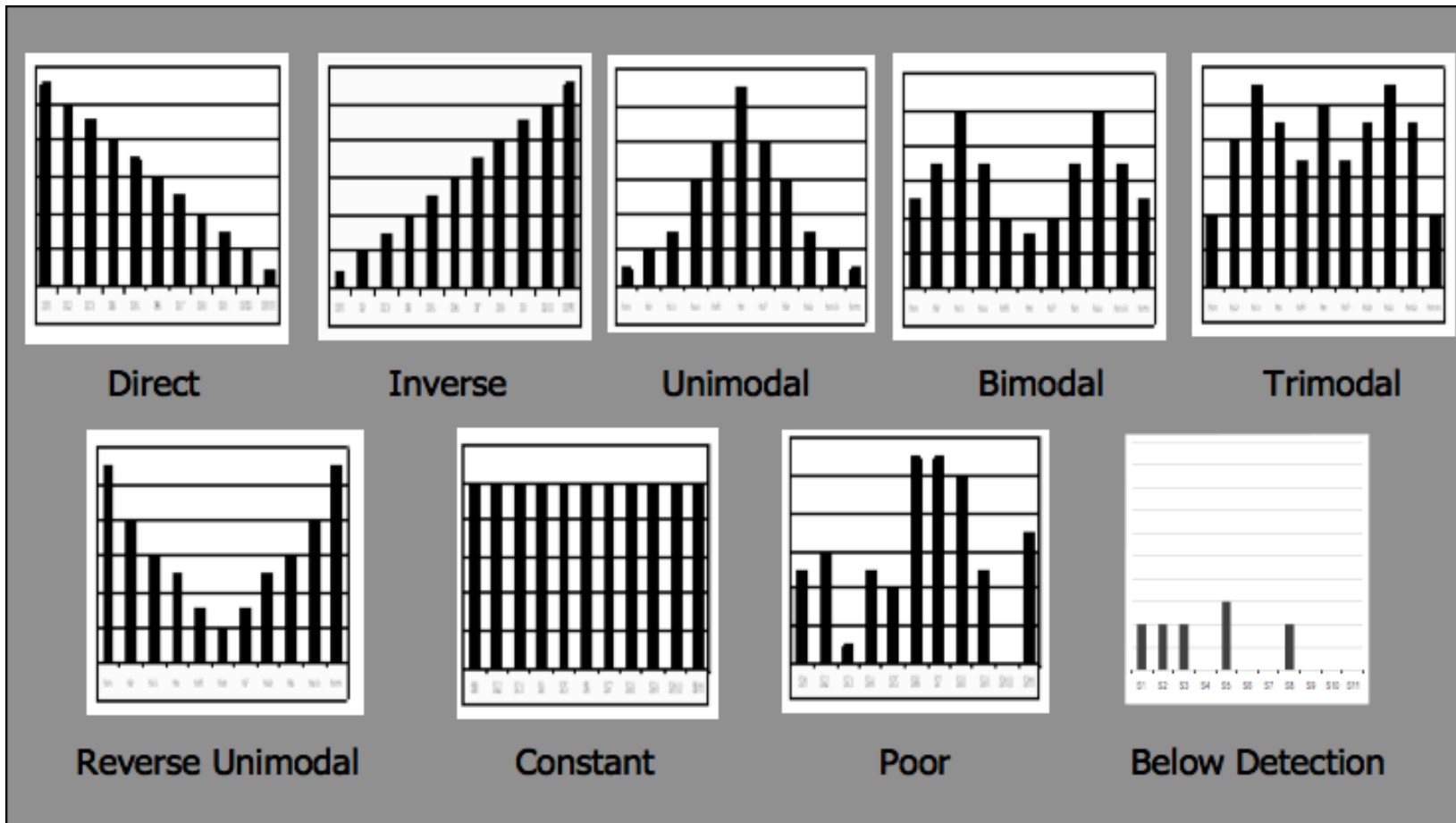


Figure 2. Schematic of different concentration trends observed within samples (particle size decreases along the X-axis from left to right; Y-axis represents concentration). Analysis of many samples indicates that the “inverse” trend between size and concentration is common for a number of heavy metals including arsenic and mercury.

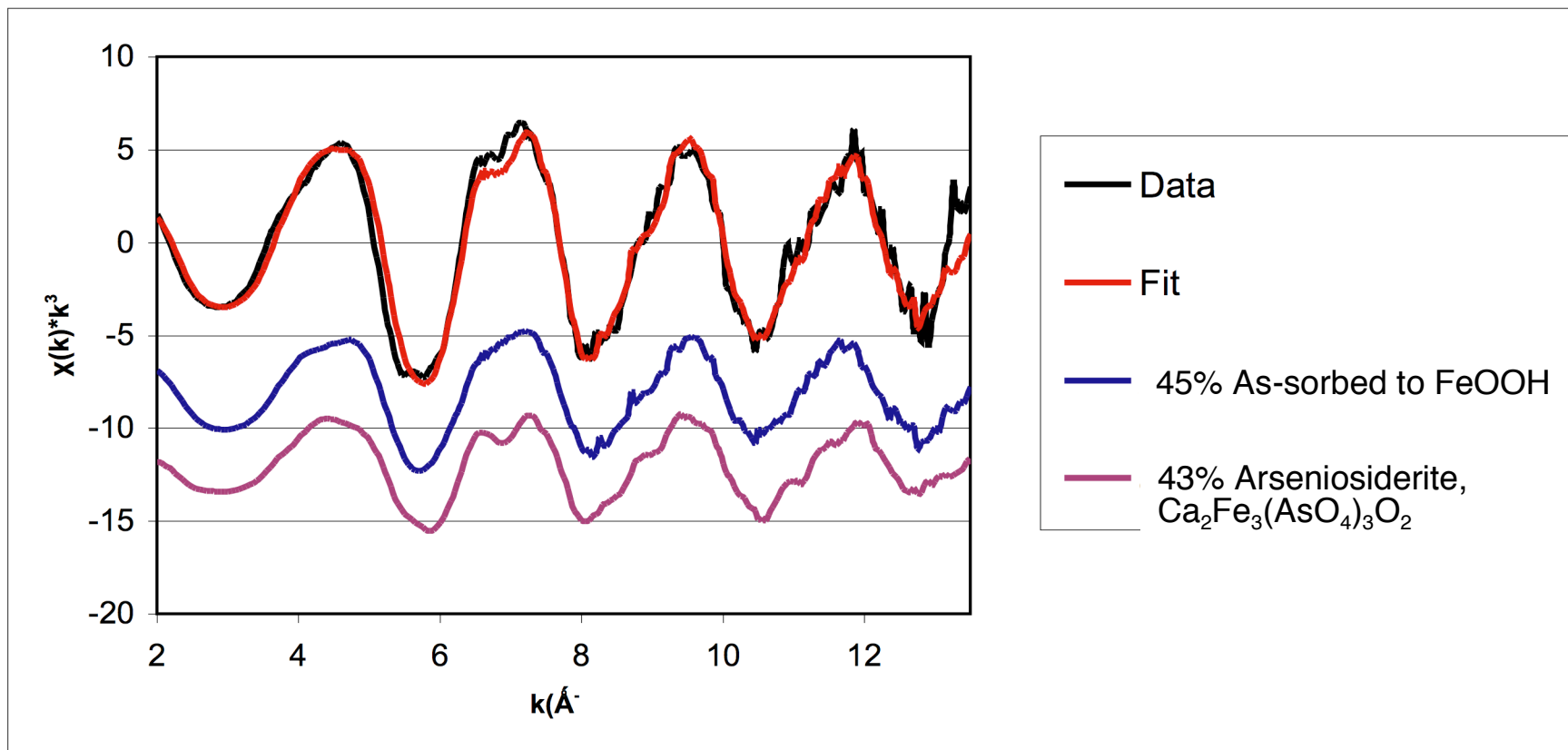


Figure 3. EXAFS speciation analysis of mine tailings sample from the Rand Mine in the Randsburg mining district.

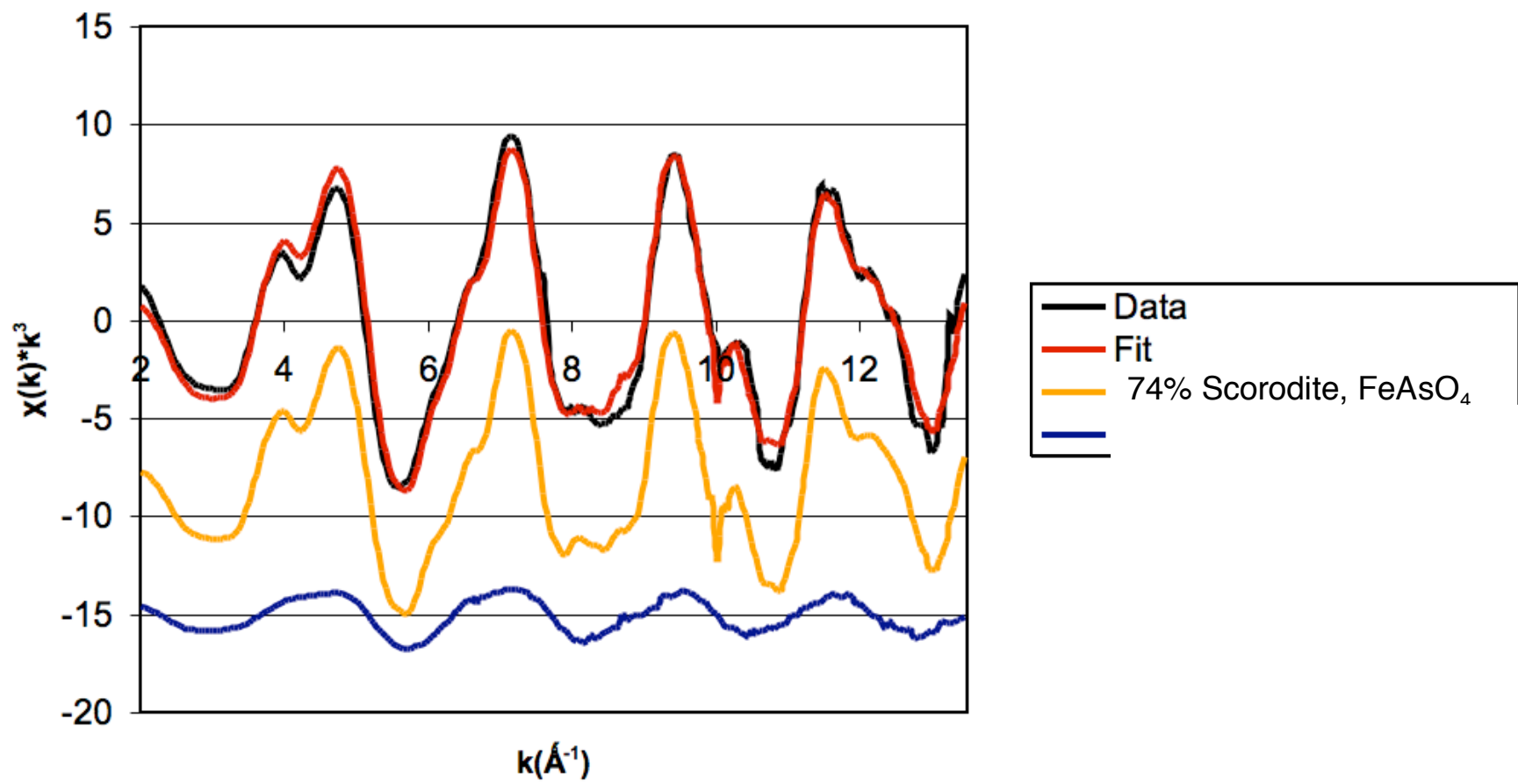


Figure 4. EXAFS speciation analysis of mine tailings sample from the Clare Mine in the Kelly mining district.

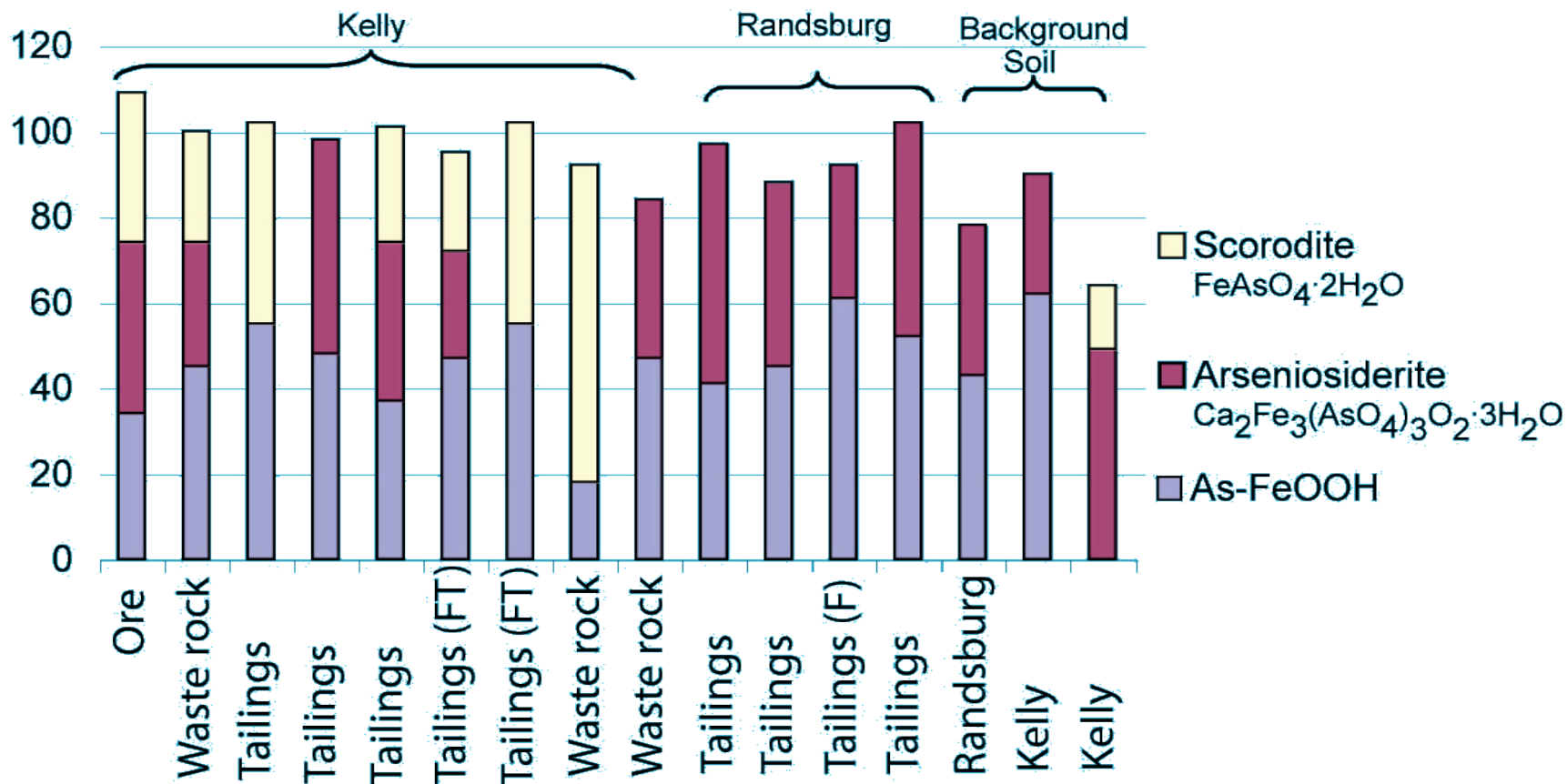


Figure 5. Speciation of samples from the Kelly and Randsburg mine regions using As K-edge EXAFS spectroscopy. (FT) = Fluvially transported tailings; (F) = Collected from air filter.

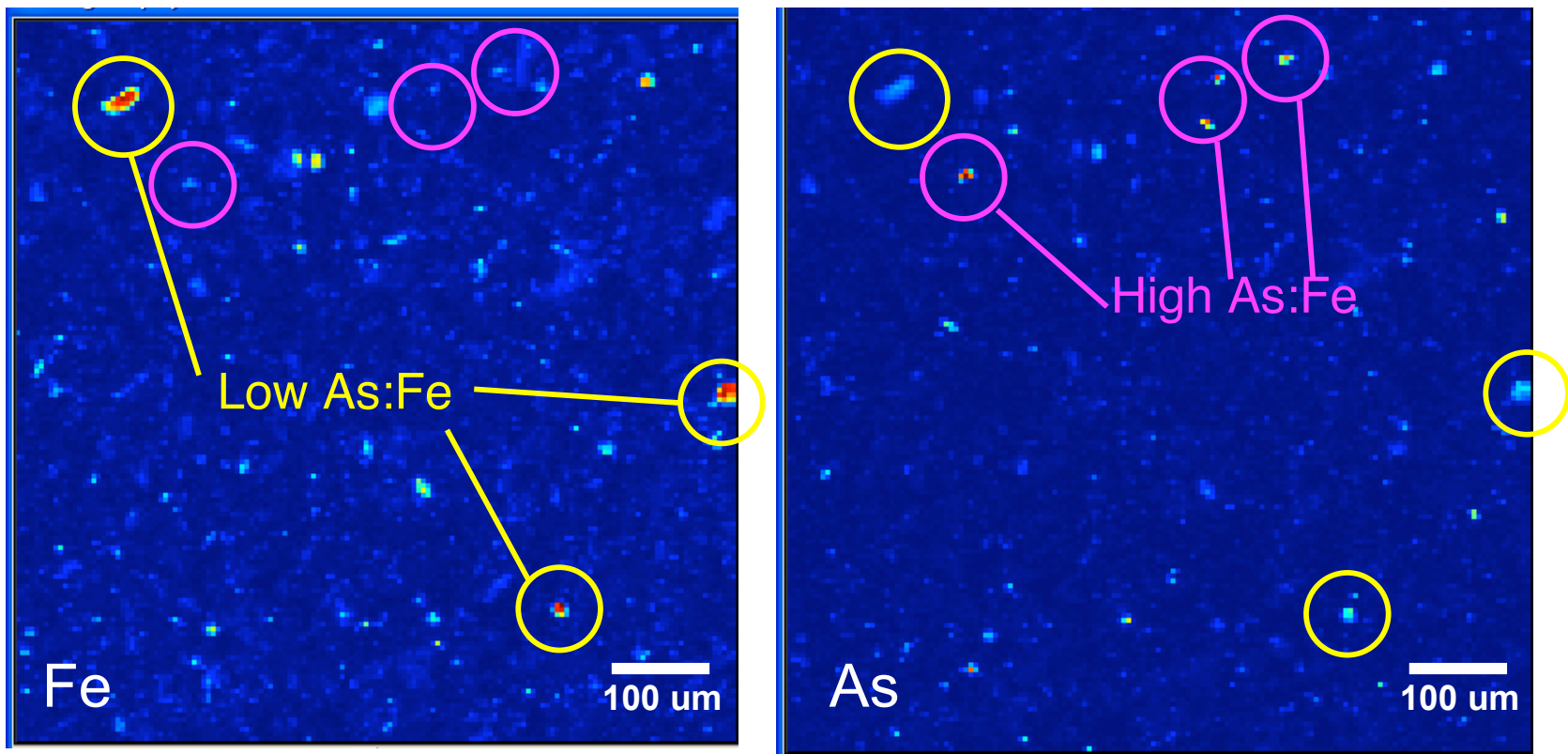


Figure 6. Iron and arsenic microscale elemental distribution maps showing two populations of particles: those with a high As:Fe ratio and those with a low As:Fe ratio. Regions encompassing particles in each population are circled on both elemental maps to aid comparison.

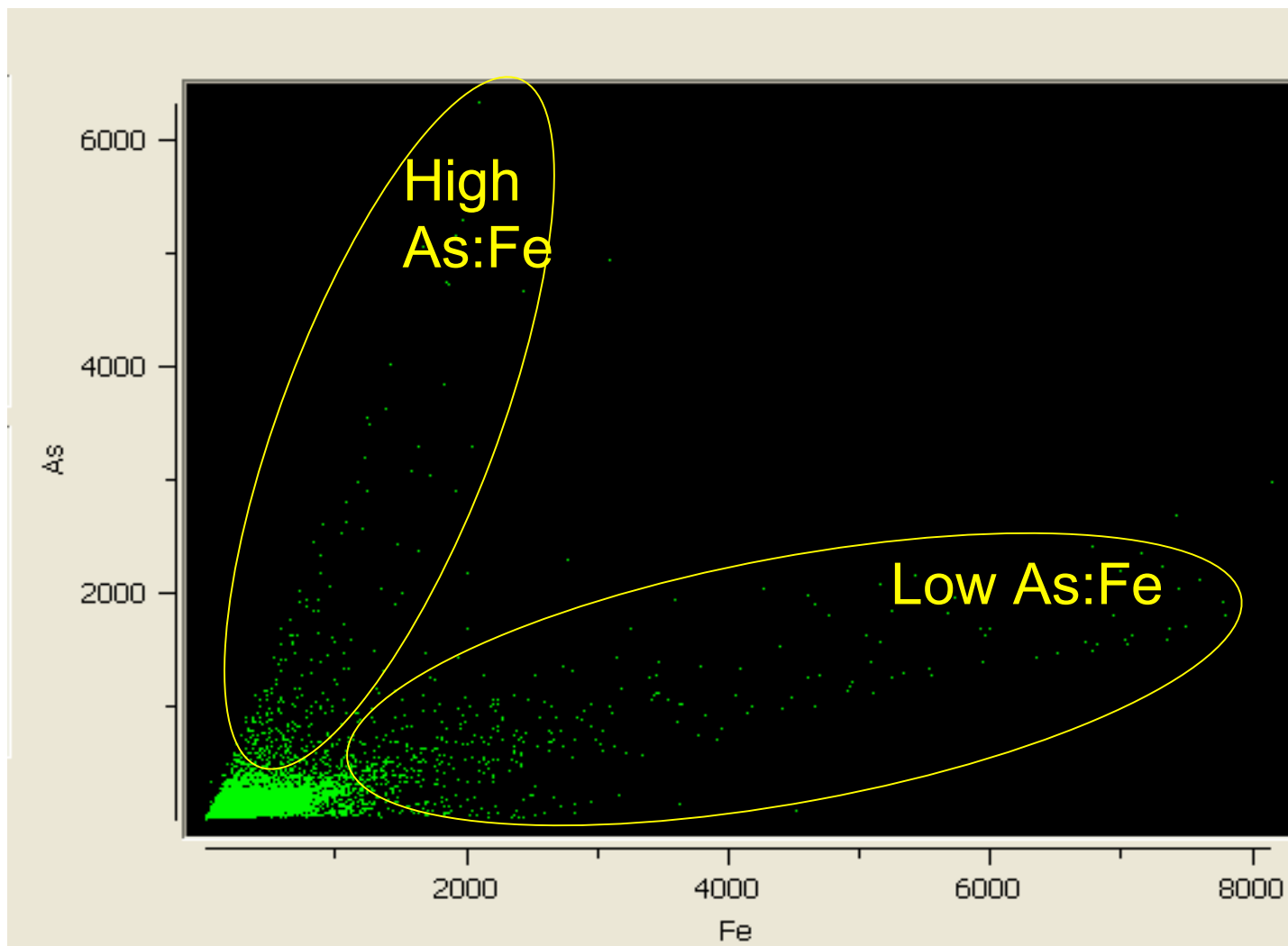


Figure 7. Correlation plot of relative fluorescence counts for As and Fe for the sample shown in Figure 6, demonstrating clearly the presence of two populations of particles where the two elements are associated with one another. Units on both axes are counts/second.

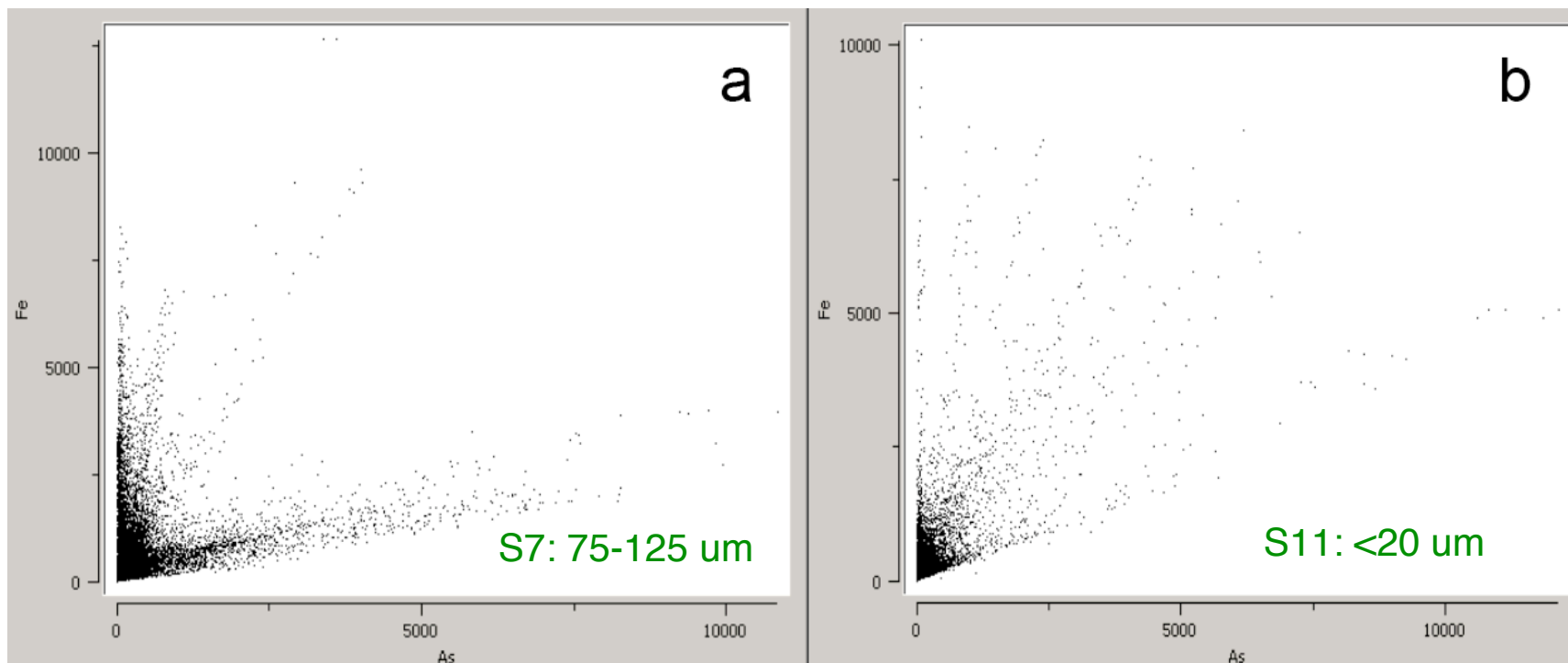


Figure 8. Comparison of As:Fe correlation plots for the S7 (a) and S11 (b) size fractions, showing an increase in diversity of particle populations with distance As:Fe ratios, suggesting a wider variety of As-bearing phases with decreasing particle size. This results in a “fingering” effect that is more apparent in the finer size fractions. Units on both axes are counts/second.

Appendix A
Inventory of size-separated samples

Dates	Sample ID	Location	Sample type	Notes
5/3/05	04RC3	Rinconada		
5/6/05	21CT50	Rinconada		
5/11/05	21CT8C	Rinconada		
7/14/05	22CC22SB	Cache Creek		No Chemex data for S9-S11
7/14/05	23CC11SB	Cache Creek		No Chemex data for S7-S11
9/14/05	05HFGPIS	Hocker Flat Pit		
7/27/06	1-3C	Kelly Mine		No Chemex data for S11
8/3/06	2-B4	Kelly Mine Pile		No Chemex data for S11
12/6/06	MG-W1	Marigold		No Chemex data for S1, S10, S11
12/13/06	06HF1053	Hocker Flat		No Chemex data for S9
12/15/06	06CC12FS	Clear Creek		
12/15/06	RBDCMT_Hill	Descarga	Tailings?	No Chemex data for S11
12/16/06	06HF12S2	Lower Hocker Flat (Randsburg)	Tailings from end of stream (highly weathered)	No Chemex data for S2 and S3
12/19/06	06JS3S2	Middle Hocker Flat (Randsburg)	Tailings from end of stream (highly weathered)	No Chemex data for S2 and S3
12/19/06	RBMT-DSGA Cliff	Descarga	Tailings?	No Chemex data for S1, S2, S10, S11
12/20/06	RBMT-YAMT1	Descarga	Tailings?	No Chemex data for S1, S2, S3, S10, S11
12/21/06	JBNE-MTW2	Johannesburg	Tailings?	No Chemex data for S10 and S11
4/17/07	07T26	Randsburg	Tailings	No Chemex data for S11
4/25/07	RMBLM-T-2-0	Red Mountain	Tailings	
5/29/07	07RMBK74	Randsburg	Background material	
5/31/07	07T66	Randsburg Solomon Mine	Tailings	
6/15/07	07BK1-0	Randsburg	Background material	
6/15/07	07-OHE-comp	Oat Hill Mine		No Chemex data for S1, S2, S10, S11
6/22/07	07T46	Randsburg	Tailings	No Chemex data for S10 and S11
6/27/07	RMS03C	Ruth Mine		
6/27/07	RMWD1/2	Ruth Mine Composite Mill	Tailings	
9/11/07	07T34	Randsburg Solomon Mine		
9/25/07	GQW-MT3	Golden Queen	Tailings	
10/2/07	GQ-MT1	Golden Queen	Tailings	
10/16/07	GQ-MT4	Golden Queen	Tailings	
10/06	06AU5F	Aurora		No Chemex data for S11
	06BC11T	Bodie Creek	Tailings?	No Chemex data for S10 and S11

Appendix B
Inventory of samples analyzed by micro-X-ray fluorescence

Dates	Elements run (channels)	Sample ID	Location	Sample type	Splits
7/20-23/2007	Fe, As, Zn, Cu, Ti, Ca, K, S, Au, Mn	OHV_FILTER	Randsburg	Dust from respirator air filter	
		07T66	Randsburg Solomon Mine	Tailings	S5,7,9,11
		07RMBK74	Randsburg	Background	S5,7,9,11
		RMBLM-T-2-0	Red Mountain	Tailings	S5,7,9,11
		RMWD1/2	Ruth Mine Composite Mill	Tailings	S5,9,11
		06BC12T	Bodie Creek	Tailings?	S9,11
4/20-23/2007	Fe, As, Zn, Cu, Ti, Ca, K, S, Mn, Hg, Ni, Se	07T26	Randsburg	Tailings	S7-11
		07BK59-1	Randsburg	Background	S7-11
		06BC11T	Bodie Creek	Tailings?	S9-11
		06AU5F	Aurora	?	S9-11
Jan-07	Fe, As, Zn, Cu, Ti, Ca, K, Mn, Hg, Ni, Se, Cl, Si, SP?	06CC12FS	Clear Creek	?	S11
		06HF12S2	Lower Hocker Flat (Randsburg)	Tailings transported to end of stream (highly weathered)	S11
		06JS3S2	Middle Hocker Flat (Randsburg)	Tailings transported to end of stream (highly weathered)	S11
		JBNE_MTW2	Johannesburg	Tailings?	S5, 9, 11
		MG_W1	Marigold	?	S7, 11
		RBDCMT_Hill	Descarga	Tailings?	S7, 9
		RBMT_DSGA Cliff	Descarga	Tailings?	S9, 11
		RBMY_YAMT1	Descarga	Tailings?	S11

Appendix C
Sample template for size separation/concentration analysis

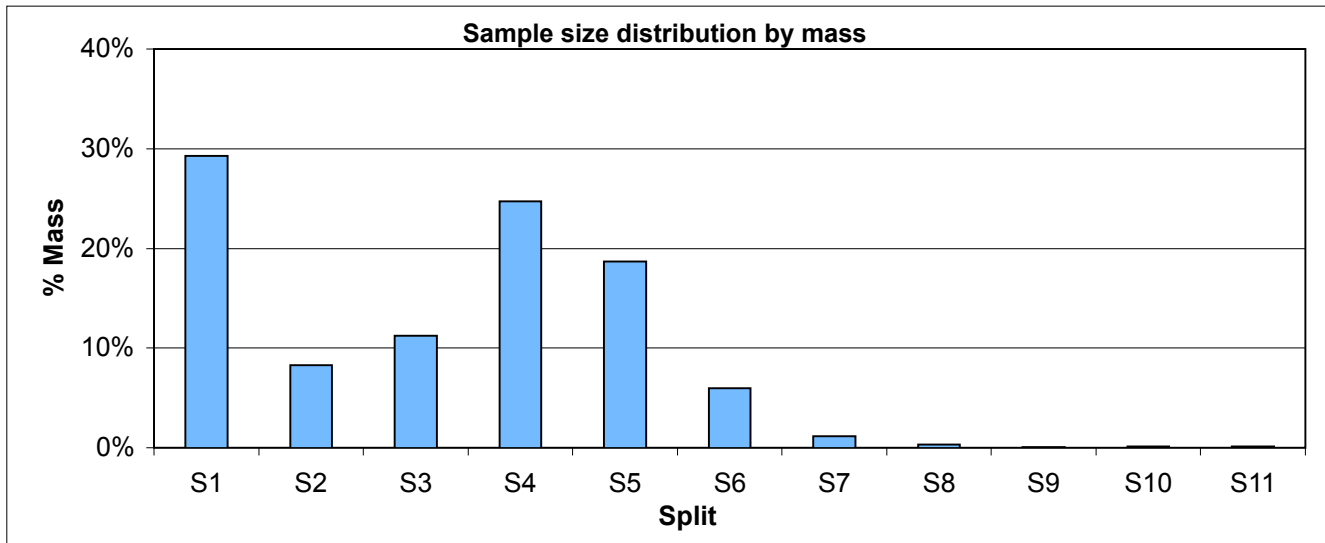
06HF1053 Sample size distribution by mass

Sample Information	
Sample ID:	06HF1053
Sample Description:	Hocker Flat
Date Sieved:	12/13/06
Name:	

Initial Mass measurement	
Trial	Mass (g)
1	385.7
2	384.4
3	393.7
4	386.4
5	397.5
6	218.7
7	297
8	290.5
9	397.4
10	901.6
Total initial mass (g):	4052.9

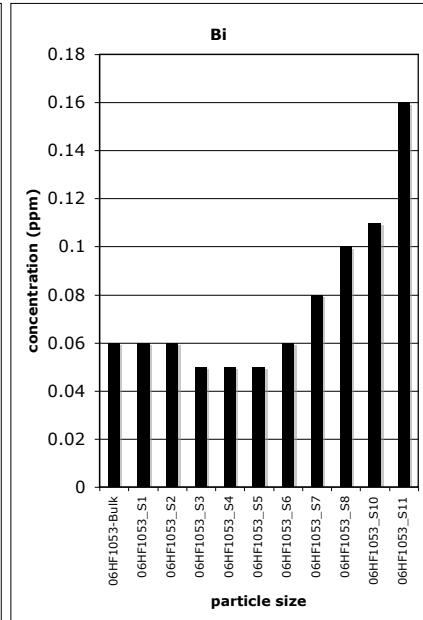
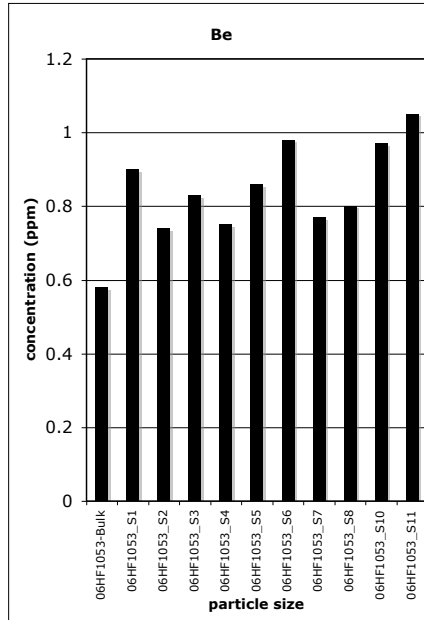
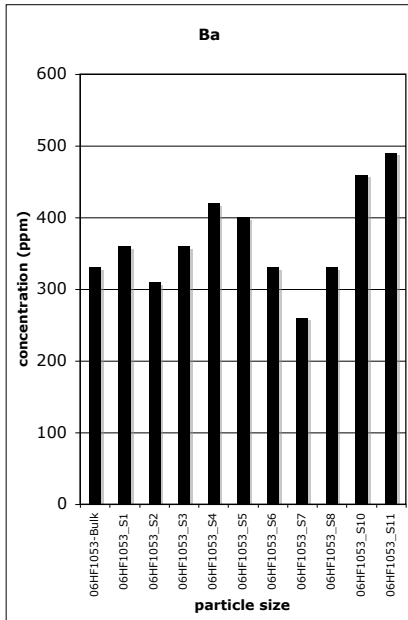
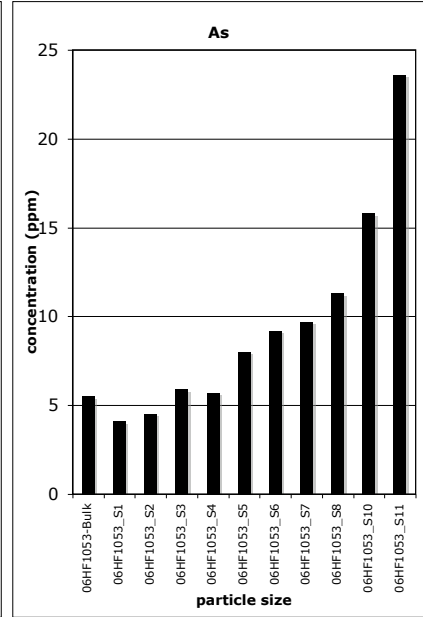
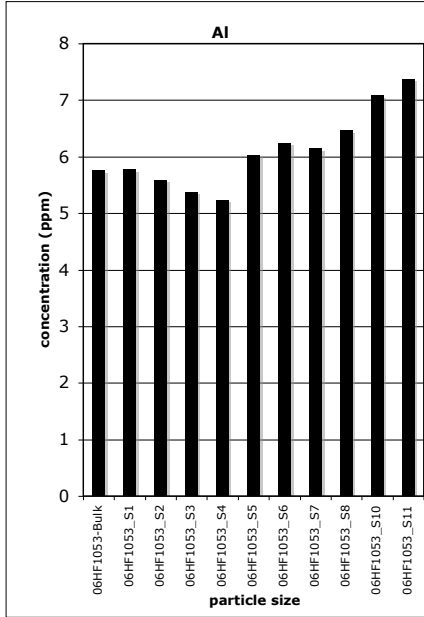
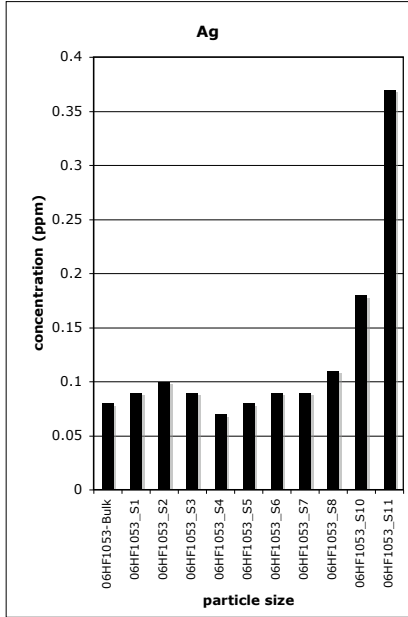
Particle Diameter (dp)	Split	% mass
dp >2830 um	S1	29.3%
2830 um>dp>1700 um	S2	8.3%
1700 um>dp>1000 um	S3	11.2%
1000 um>dp>500 um	S4	24.7%
500 um>dp>250 um	S5	18.7%
250 um>dp>125 um	S6	6.0%
125 um>dp>75 um	S7	1.2%
75 um>dp>45 um	S8	0.3%
45 um>dp>32 um	S9	0.1%
32 um>dp>20 um	S10	0.1%
dp<20 um	S11	0.2%

Sample split information		
06HF1053 S1 dp >2830 um 1161.7 g 580.85 g (split)	06HF1053 S6 250 um>dp>125 um 237.7 g 118.85 g (split)	
06HF1053 S2 2830 um>dp>1700 um 328.4 g 164.2 g (split)	06HF1053 S7 125 um>dp>75 um 46.1 g 23.05 g (split)	
06HF1053 S3 1700 um>dp>1000 um 446.7 g 223.35 g (split)	06HF1053 S8 75 um>dp>45 um 13.6 g NSS g (split)	
06HF1053 S4 1000 um>dp>500 um 981.2 g 490.6 g (split)	06HF1053 S9 45 um>dp>32 um 3.7 g NSS g (split)	
06HF1053 S5 500 um>dp>250 um 741.8 g 370.9 g (split)	06HF1053 S10 32 um>dp>20 um 4.2 g NSS g (split)	
Sum of splits % error	3971.2 g 2.0%	06HF1053 S11 dp<20 um 6.1 g NSS g (split)



Elemental Distribution (by Concentration) vs. Particle Size

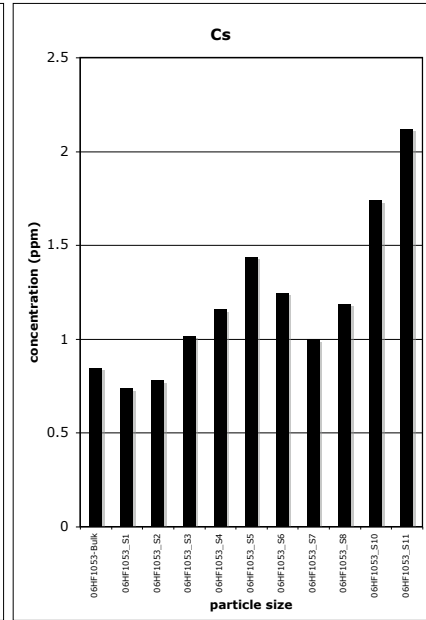
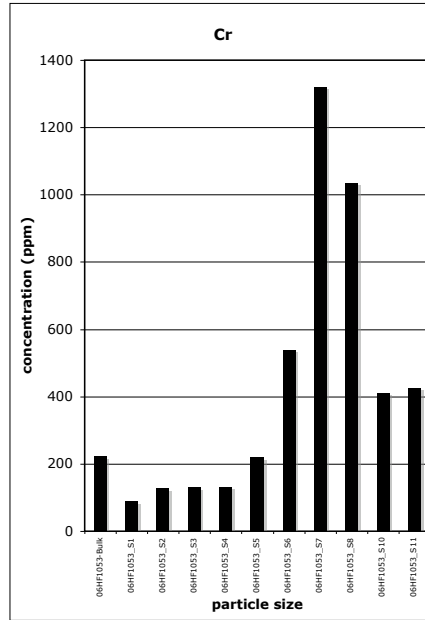
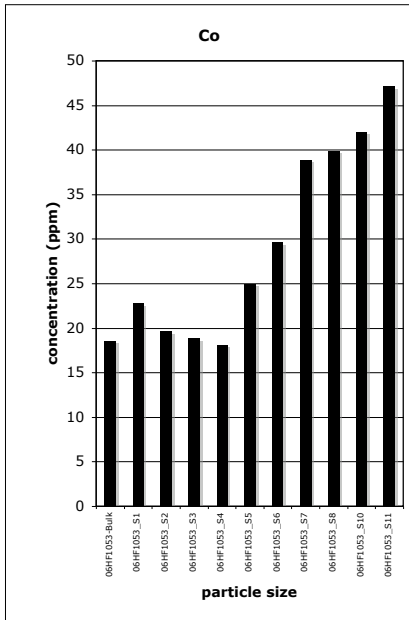
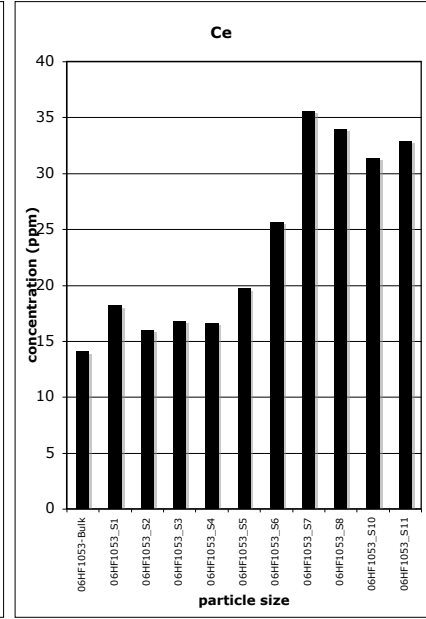
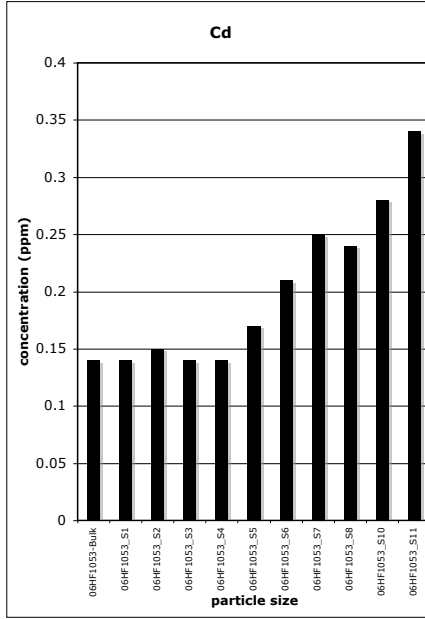
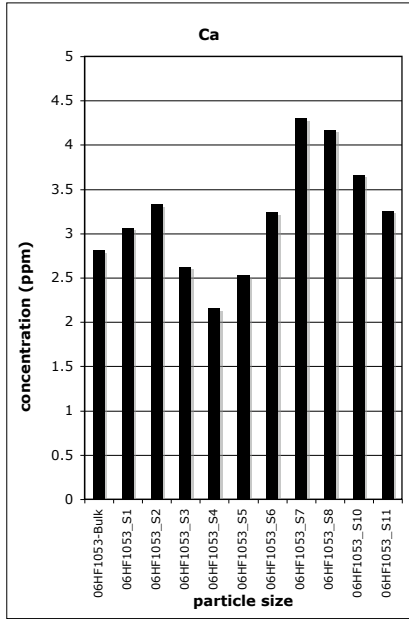
SAMPLE DESCRIPTION	WEI-21 Recvd Wt. kg	ME-MS61 Ag ppm	ME-MS61 Al %	ME-MS61 As ppm	ME-MS61 Ba ppm	ME-MS61 Be ppm	ME-MS61 Bi ppm
06HF1053-Bulk	0.08	0.08	5.76	5.5	330	0.58	0.06
06HF1053_S1	0.06	0.09	5.77	4.1	360	0.9	0.06
06HF1053_S2	0.18	0.1	5.59	4.5	310	0.74	0.06
06HF1053_S3	0.06	0.09	5.37	5.9	360	0.83	0.05
06HF1053_S4	0.08	0.07	5.24	5.7	420	0.75	0.05
06HF1053_S5	0.08	0.08	6.03	8	400	0.86	0.05
06HF1053_S6	0.16	0.09	6.25	9.2	330	0.98	0.06
06HF1053_S7	0.04	0.09	6.14	9.7	260	0.77	0.08
06HF1053_S8	0.02	0.11	6.46	11.3	330	0.8	0.1
06HF1053_S10	0.02	0.18	7.08	15.8	460	0.97	0.11
06HF1053_S11	0.02	0.37	7.38	23.6	490	1.05	0.16



S1> 2830 um	1000 um>S4>500 um	125 um>S7>75 um	32 um>S10>20 um
2830 um>S2>1700 um	500 um>S5>250 um	75 um>S8>45 um	20 um>S11
1700 um>S3>1000 um	250 um>S6>125 um	45 um>S9>32 um	

Elemental Distribution (by Concentration) vs. Particle Size

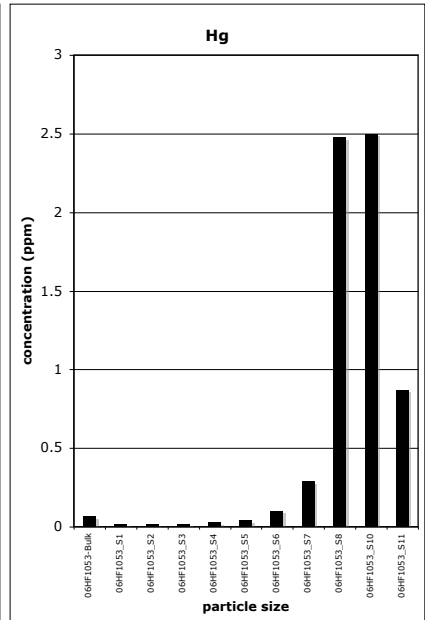
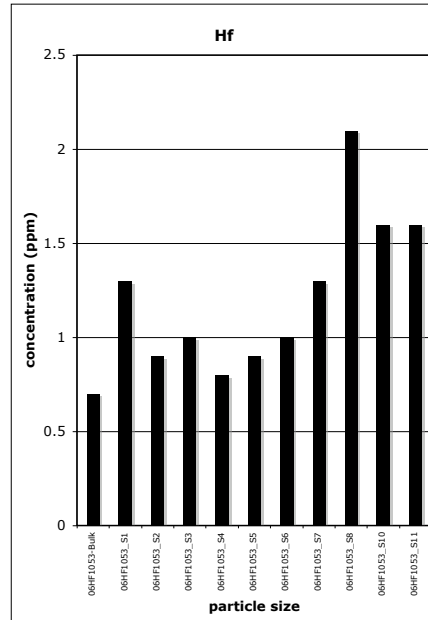
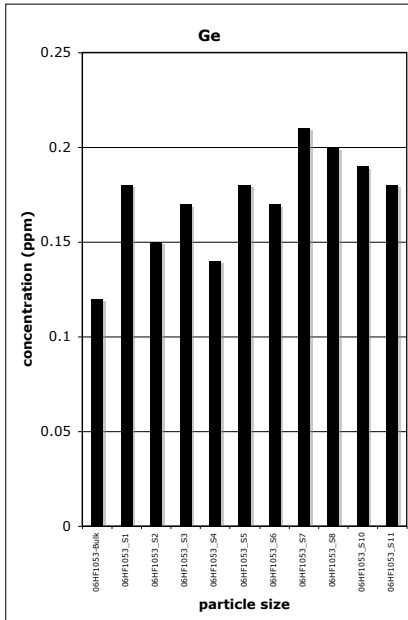
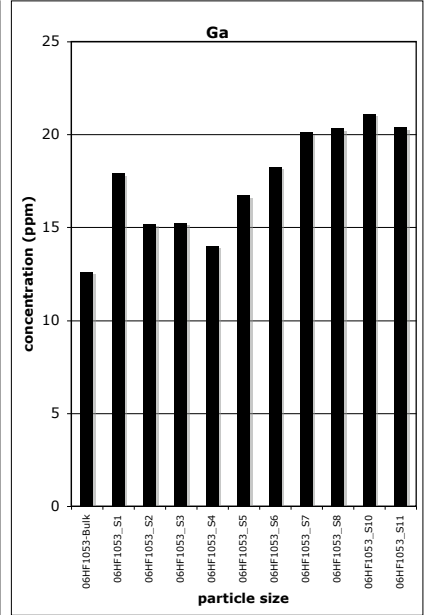
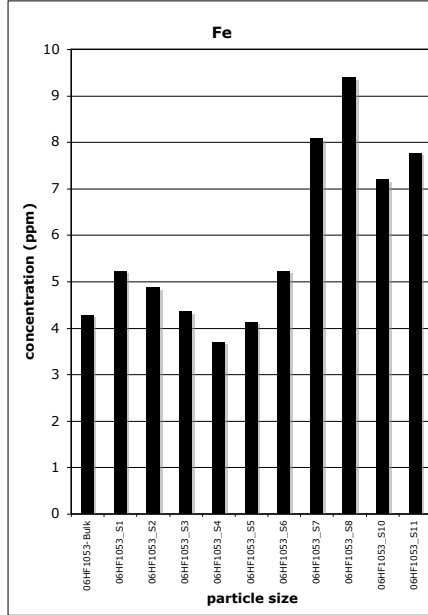
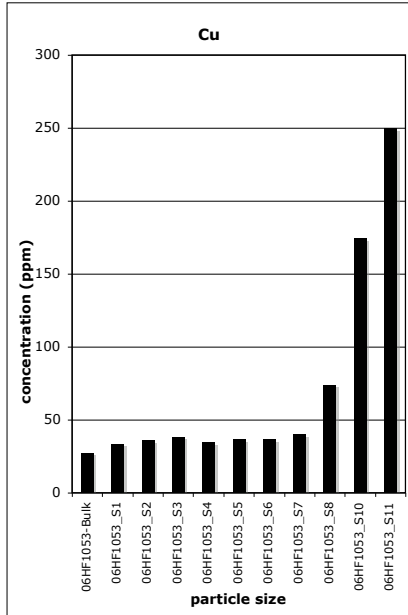
ME-MS61 Ca %	ME-MS61 Cd ppm	ME-MS61 Ce ppm	ME-MS61 Co ppm	ME-MS61 Cr ppm	ME-MS61 Cs ppm
2.81	0.14	14.1	18.5	223	0.85
3.06	0.14	18.2	22.8	88	0.74
3.33	0.15	16	19.6	127	0.78
2.62	0.14	16.8	18.8	130	1.02
2.15	0.14	16.65	18.1	132	1.16
2.53	0.17	19.75	24.9	219	1.44
3.24	0.21	25.7	29.6	538	1.25
4.3	0.25	35.6	38.9	1320	1
4.17	0.24	34	39.9	1035	1.19
3.66	0.28	31.4	42	411	1.74
3.26	0.34	32.9	47.1	426	2.12



S1> 2830 um	1000 um>S4>500 um	125 um>S7>75 um	32 um>S10>20 um
2830 um>S2>1700 um	500 um>S5>250 um	75 um>S8>45 um	20 um>S11
1700 um>S3>1000 um	250 um>S6>125 um	45 um>S9>32 um	

Elemental Distribution (by Concentration) vs. Particle Size

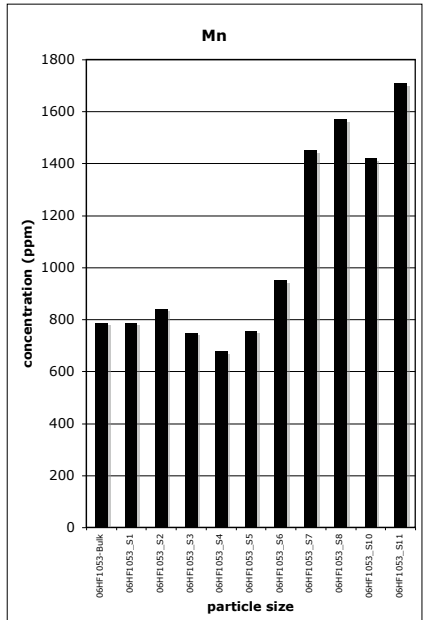
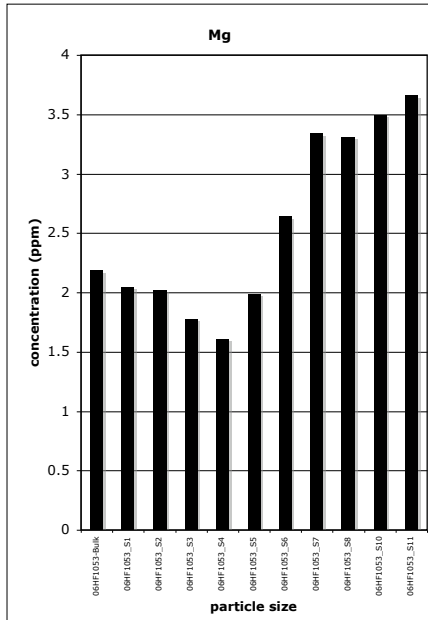
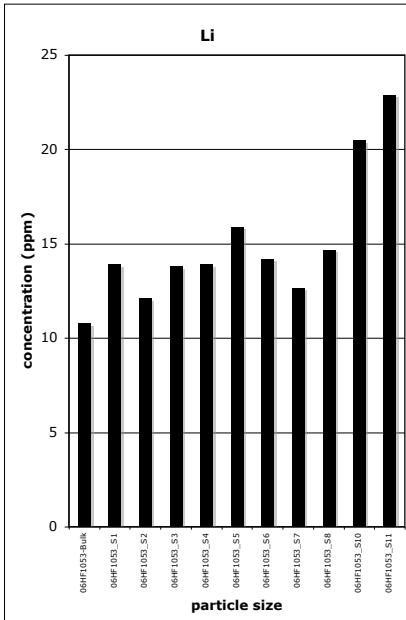
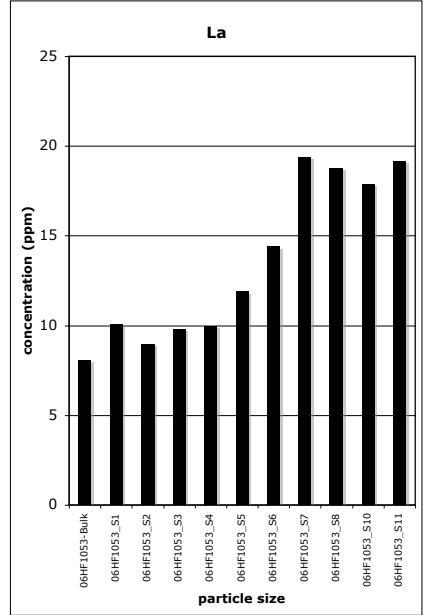
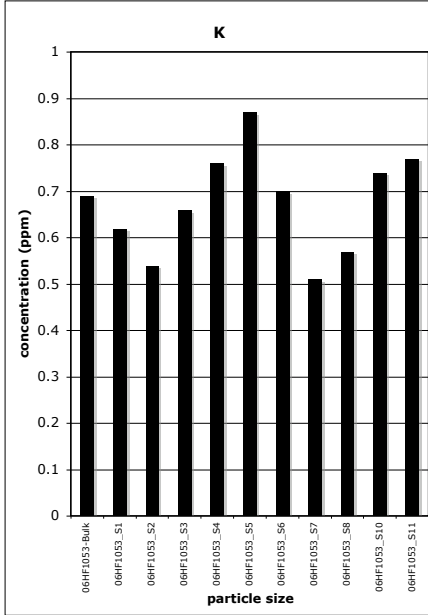
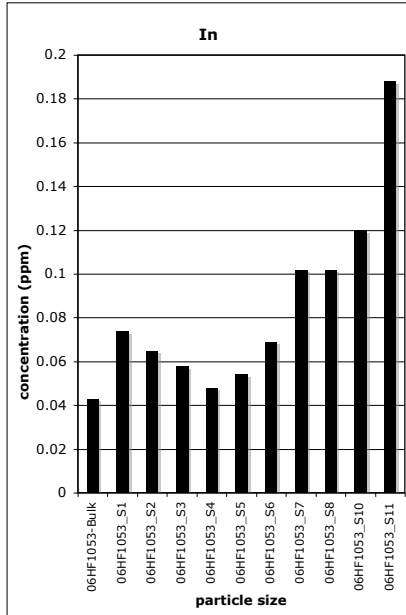
ME-MS61 Cu ppm	ME-MS61 Fe %	ME-MS61 Ga ppm	ME-MS61 Ge ppm	ME-MS61 Hf ppm	Hg-CV42 Hg ppm
27.7	4.29	12.6	0.12	0.7	0.07
33.8	5.23	17.9	0.18	1.3	0.02
35.9	4.87	15.2	0.15	0.9	0.02
38.4	4.36	15.25	0.17	1	0.02
34.5	3.71	14	0.14	0.8	0.03
36.9	4.13	16.75	0.18	0.9	0.04
36.7	5.24	18.25	0.17	1	0.1
40.2	8.08	20.1	0.21	1.3	0.29
74	9.39	20.3	0.2	2.1	2.48
174.5	7.21	21.1	0.19	1.6	2.5
250	7.77	20.4	0.18	1.6	0.87



S1 > 2830 um	1000 um > S4 > 500 um	125 um > S7 > 75 um	32 um > S10 > 20 um
2830 um > S2 > 1700 um	500 um > S5 > 250 um	75 um > S8 > 45 um	20 um > S11
1700 um > S3 > 1000 um	250 um > S6 > 125 um	45 um > S9 > 32 um	

Elemental Distribution (by Concentration) vs. Particle Size

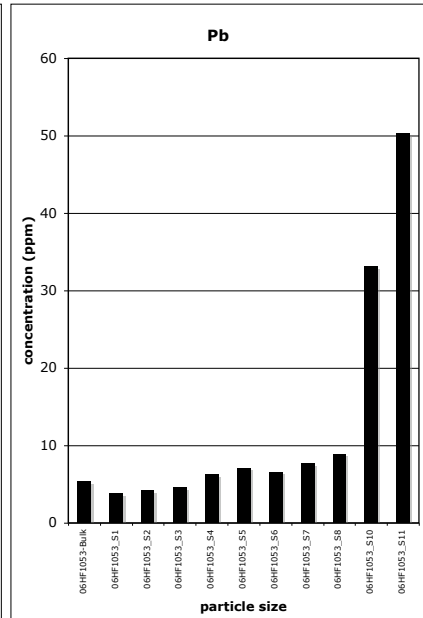
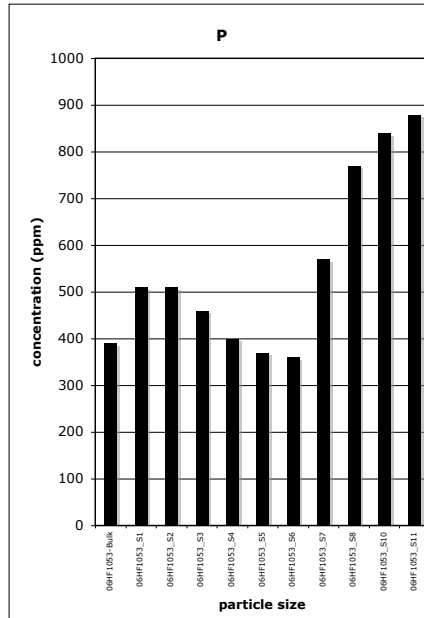
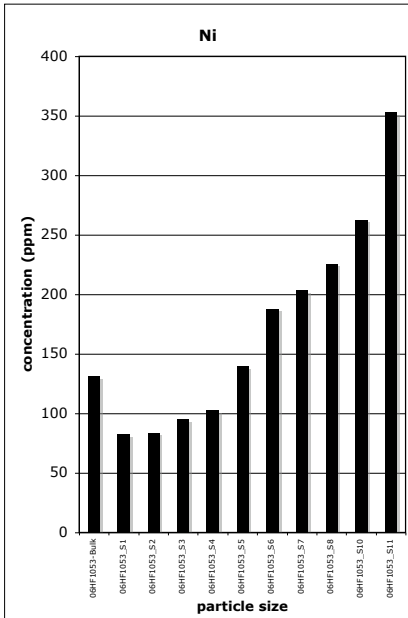
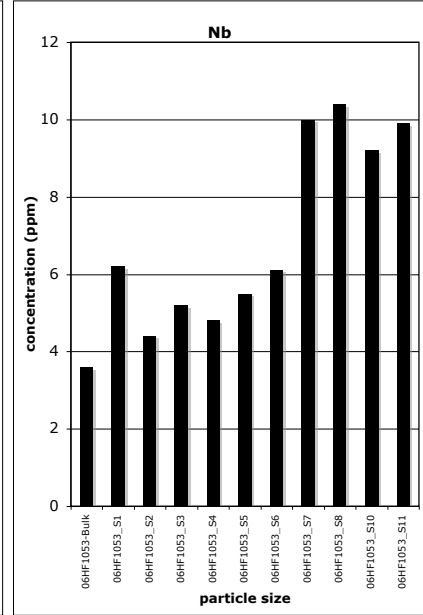
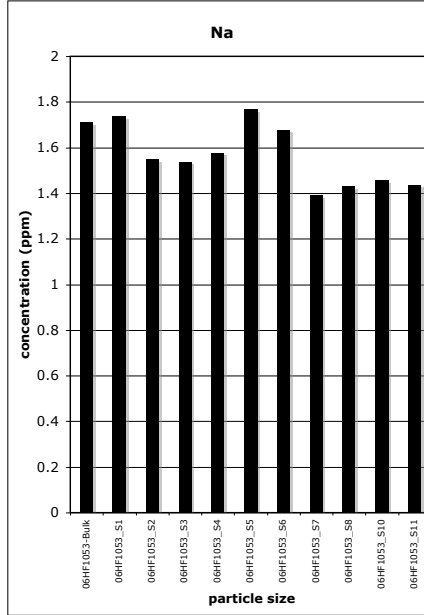
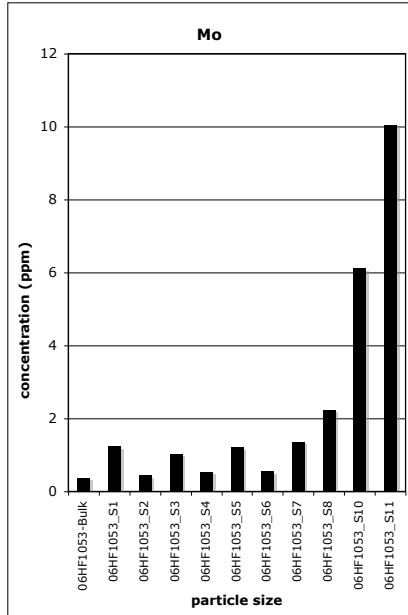
ME-MS61 In ppm	ME-MS61 K %	ME-MS61 La ppm	ME-MS61 Li ppm	ME-MS61 Mg %	ME-MS61 Mn ppm
0.043	0.69	8.1	10.8	2.19	789
0.074	0.62	10.1	13.9	2.05	787
0.065	0.54	9	12.1	2.02	843
0.058	0.66	9.8	13.8	1.78	749
0.048	0.76	10	13.9	1.61	678
0.054	0.87	11.9	15.9	1.99	757
0.069	0.7	14.4	14.2	2.64	951
0.102	0.51	19.4	12.7	3.34	1450
0.102	0.57	18.8	14.7	3.31	1570
0.12	0.74	17.9	20.5	3.5	1420
0.188	0.77	19.2	22.9	3.66	1710



S1 > 2830 um	1000 um > S4 > 500 um	125 um > S7 > 75 um	32 um > S10 > 20 um
2830 um > S2 > 1700 um	500 um > S5 > 250 um	75 um > S8 > 45 um	20 um > S11
1700 um > S3 > 1000 um	250 um > S6 > 125 um	45 um > S9 > 32 um	

Elemental Distribution (by Concentration) vs. Particle Size

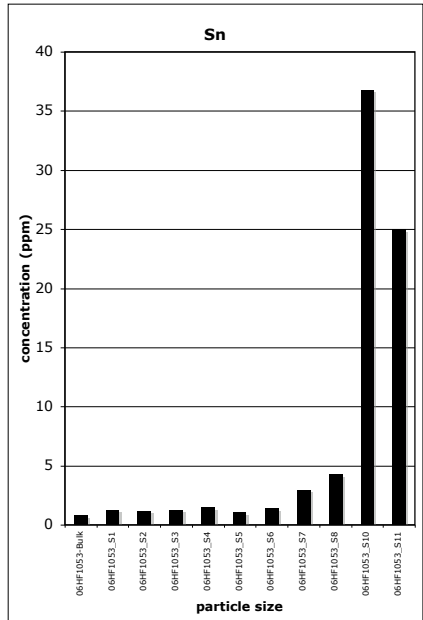
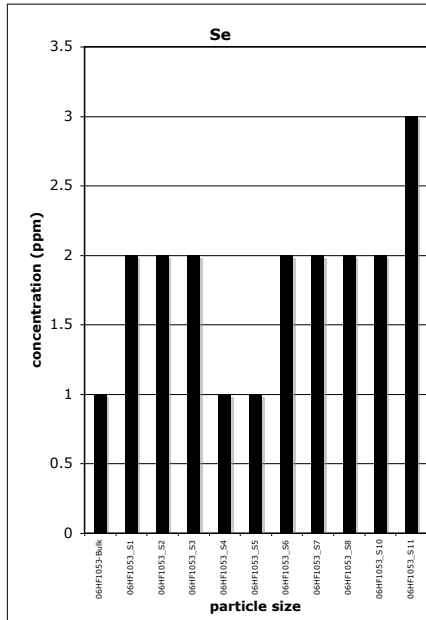
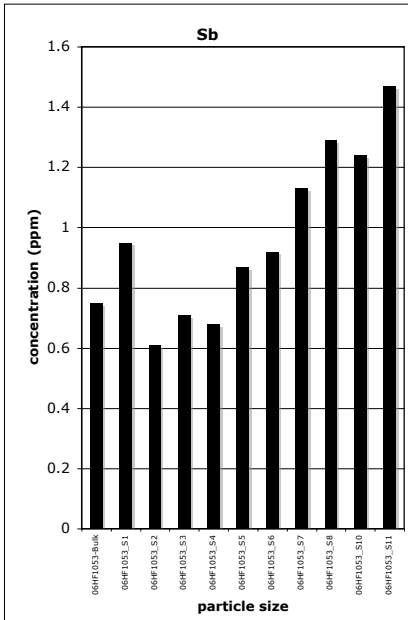
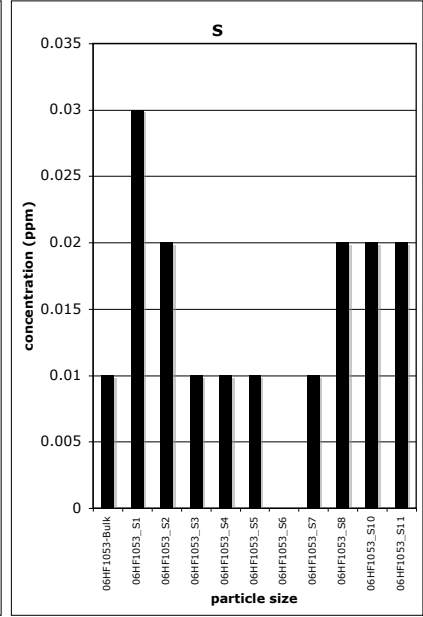
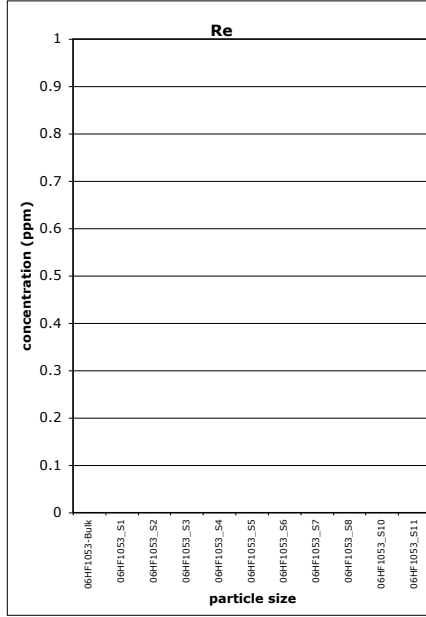
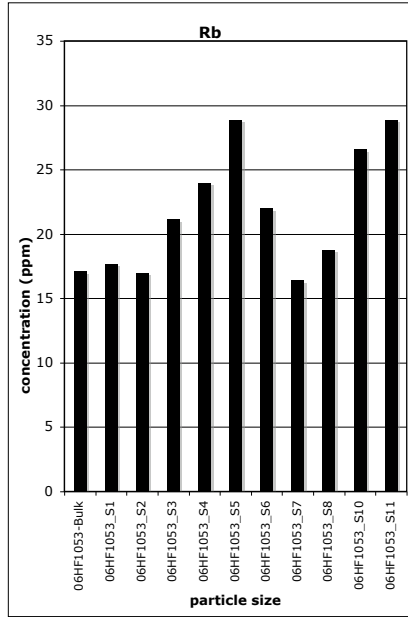
ME-MS61 Mo ppm	ME-MS61 Na %	ME-MS61 Nb ppm	ME-MS61 Ni ppm	ME-MS61 P ppm	ME-MS61 Pb ppm
0.38	1.71	3.6	131	390	5.4
1.24	1.74	6.2	82.8	510	3.8
0.46	1.55	4.4	83.9	510	4.2
1.03	1.54	5.2	95.3	460	4.6
0.55	1.58	4.8	102.5	400	6.3
1.21	1.77	5.5	140	370	7.1
0.57	1.68	6.1	188	360	6.6
1.37	1.39	10	204	570	7.7
2.25	1.43	10.4	226	770	8.9
6.12	1.46	9.2	263	840	33.1
10.05	1.44	9.9	353	880	50.3



S1> 2830 um	1000 um>S4>500 um	125 um>S7>75 um	32 um>S10>20 um
2830 um>S2>1700 um	500 um>S5>250 um	75 um>S8>45 um	20 um>S11
1700 um>S3>1000 um	250 um>S6>125 um	45 um>S9>32 um	

Elemental Distribution (by Concentration) vs. Particle Size

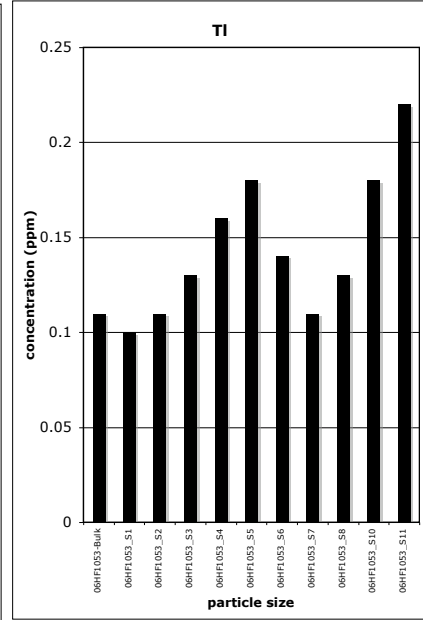
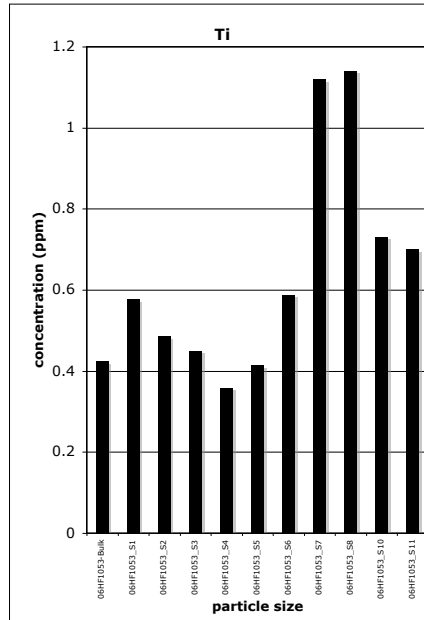
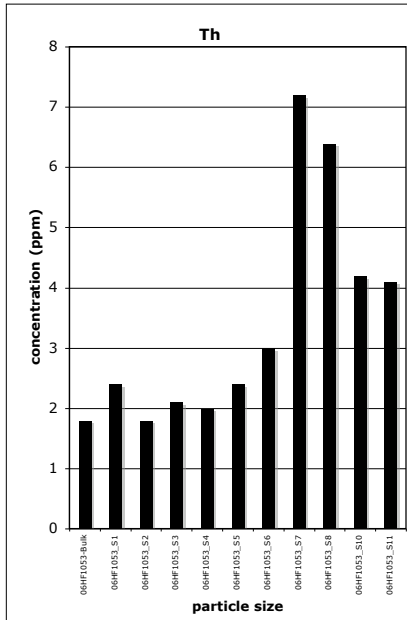
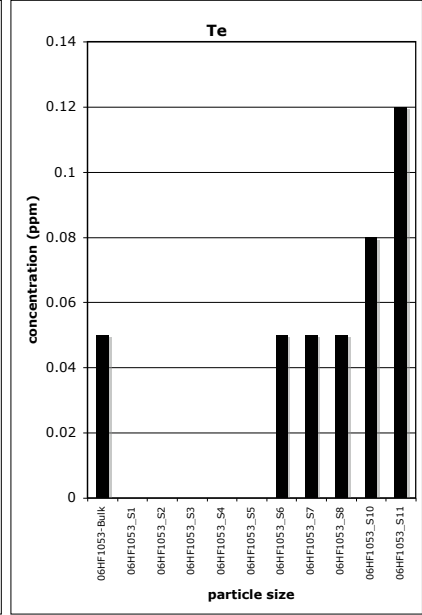
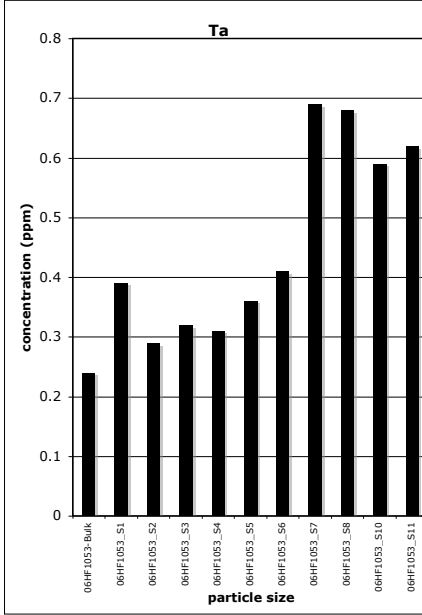
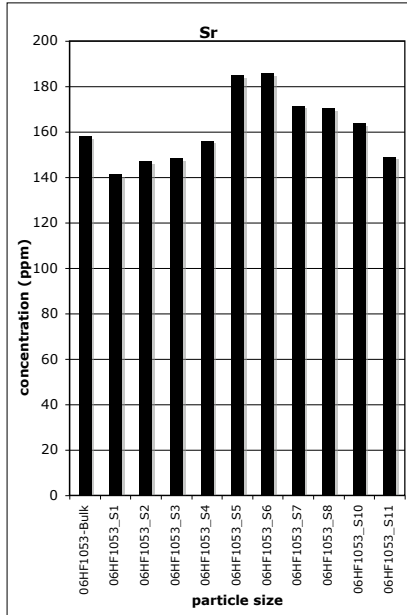
ME-MS61 Rb ppm	ME-MS61 Re ppm	ME-MS61 S %	ME-MS61 Sb ppm	ME-MS61 Se ppm	ME-MS61 Sn ppm
17.1	<0.002	0.01	0.75	1	0.8
17.7	<0.002	0.03	0.95	2	1.3
17	<0.002	0.02	0.61	2	1.2
21.2	<0.002	0.01	0.71	2	1.3
24	<0.002	0.01	0.68	1	1.5
28.9	<0.002	0.01	0.87	1	1.1
22	<0.002	<0.01	0.92	2	1.4
16.4	<0.002	0.01	1.13	2	3
18.8	<0.002	0.02	1.29	2	4.3
26.6	<0.002	0.02	1.24	2	36.8
28.9	<0.002	0.02	1.47	3	25



S1 > 2830 um	1000 um > S4 > 500 um	125 um > S7 > 75 um	32 um > S10 > 20 um
2830 um > S2 > 1700 um	500 um > S5 > 250 um	75 um > S8 > 45 um	20 um > S11
1700 um > S3 > 1000 um	250 um > S6 > 125 um	45 um > S9 > 32 um	

Elemental Distribution (by Concentration) vs. Particle Size

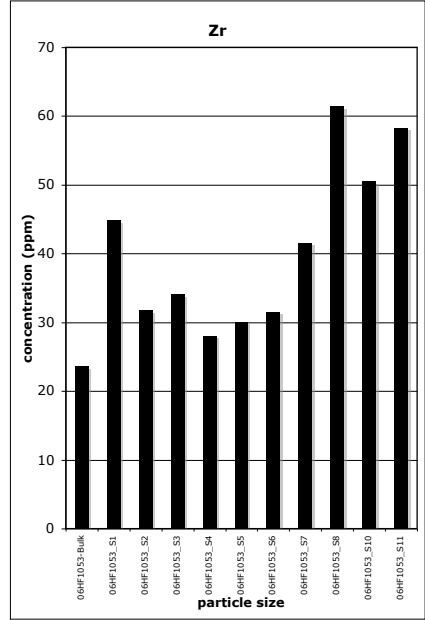
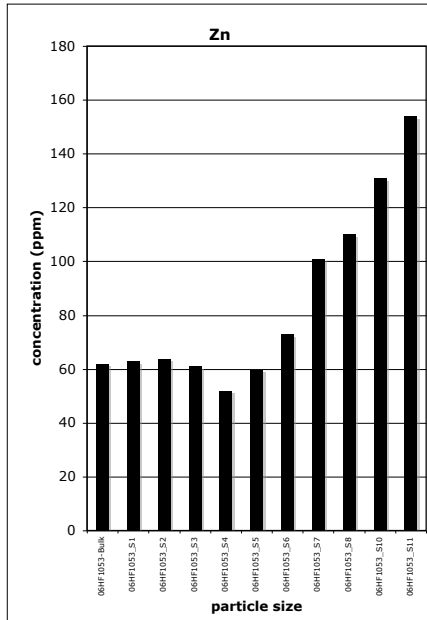
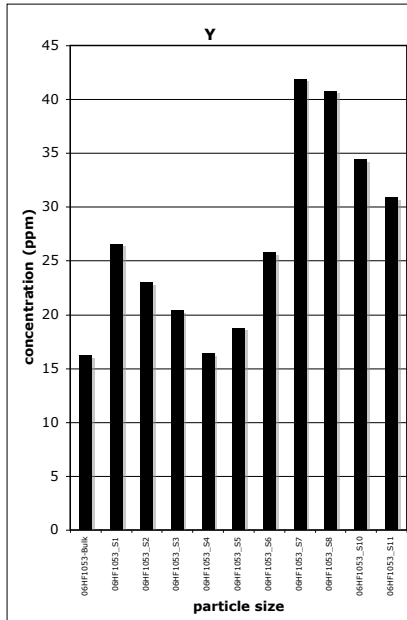
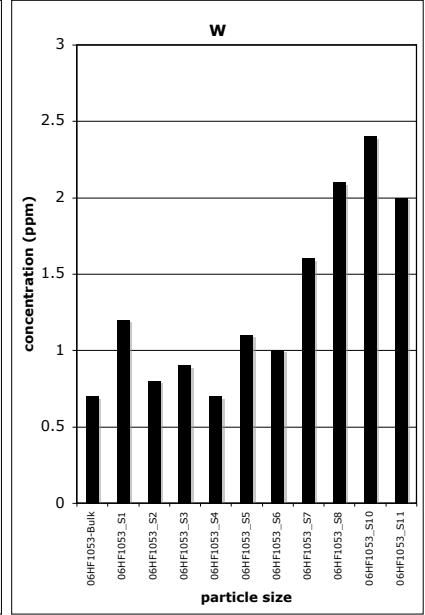
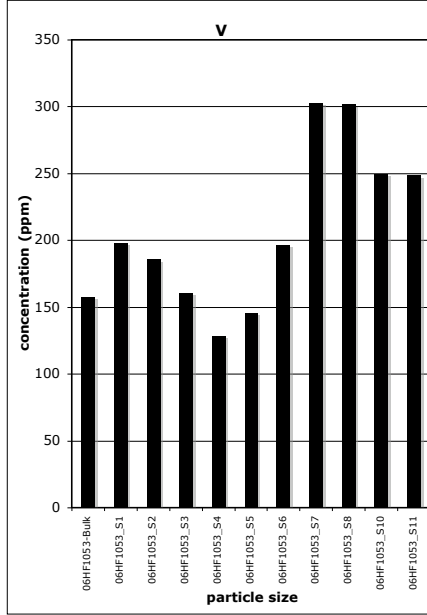
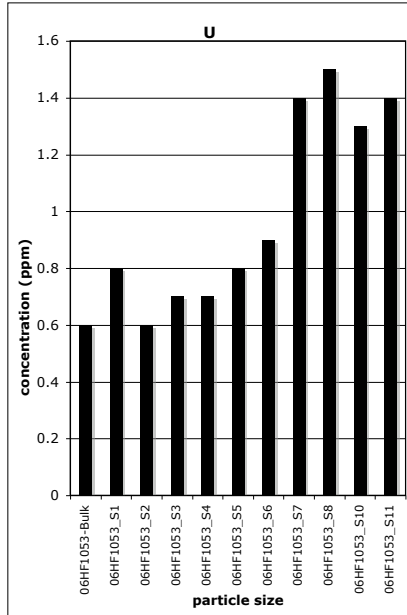
ME-MS61 Sr ppm	ME-MS61 Ta ppm	ME-MS61 Te ppm	ME-MS61 Th ppm	ME-MS61 Ti %	ME-MS61 Tl ppm
158	0.24	0.05	1.8	0.423	0.11
141.5	0.39	<0.05	2.4	0.577	0.1
147	0.29	<0.05	1.8	0.485	0.11
148.5	0.32	<0.05	2.1	0.45	0.13
156	0.31	<0.05	2	0.359	0.16
185	0.36	<0.05	2.4	0.414	0.18
186	0.41	0.05	3	0.587	0.14
171.5	0.69	0.05	7.2	1.12	0.11
170.5	0.68	0.05	6.4	1.14	0.13
164	0.59	0.08	4.2	0.731	0.18
149	0.62	0.12	4.1	0.7	0.22



S1> 2830 um	1000 um>S4>500 um	125 um>S7>75 um	32 um>S10>20 um
2830 um>S2>1700 um	500 um>S5>250 um	75 um>S8>45 um	20 um>S11
1700 um>S3>1000 um	250 um>S6>125 um	45 um>S9>32 um	

Elemental Distribution (by Concentration) vs. Particle Size

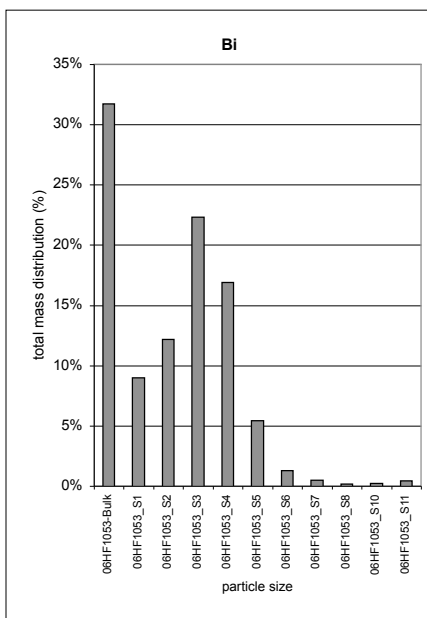
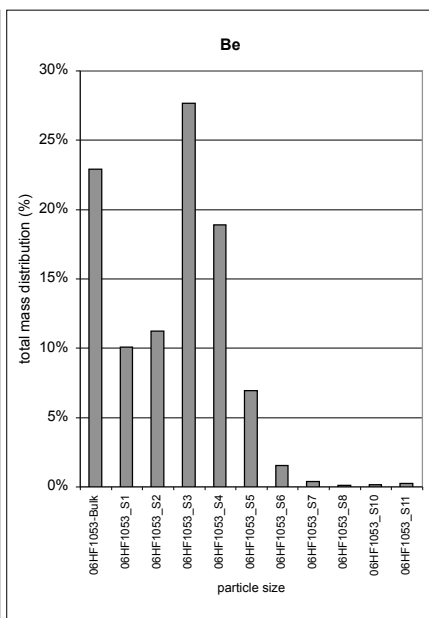
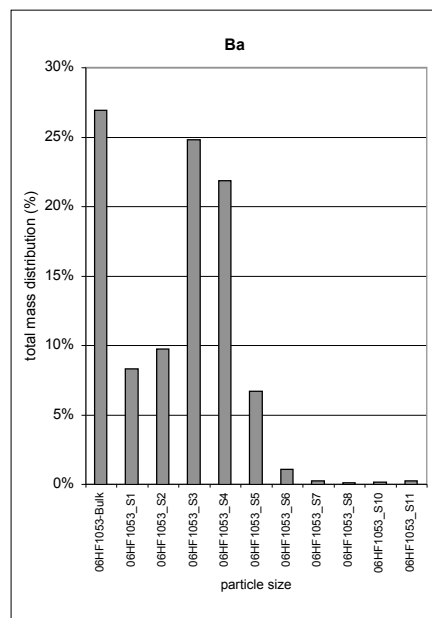
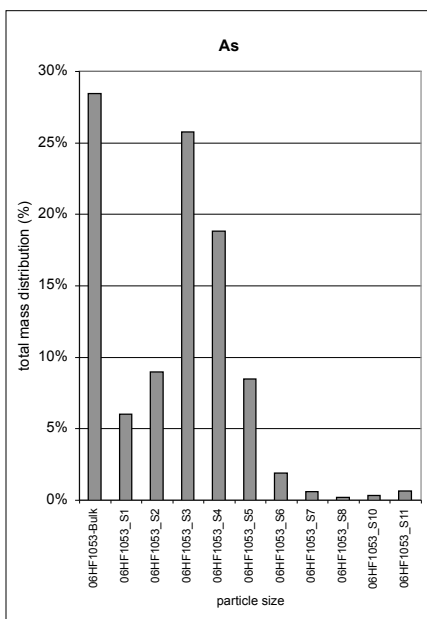
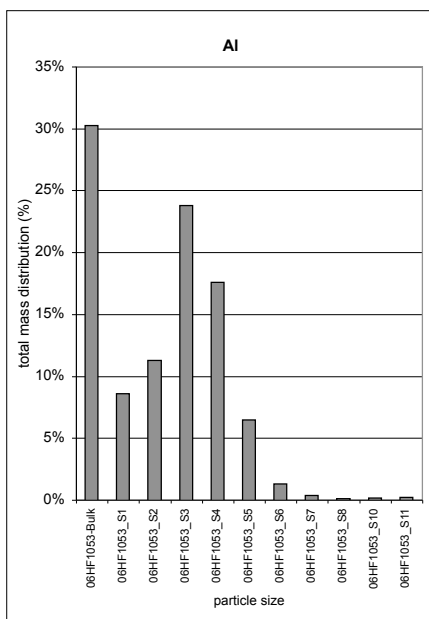
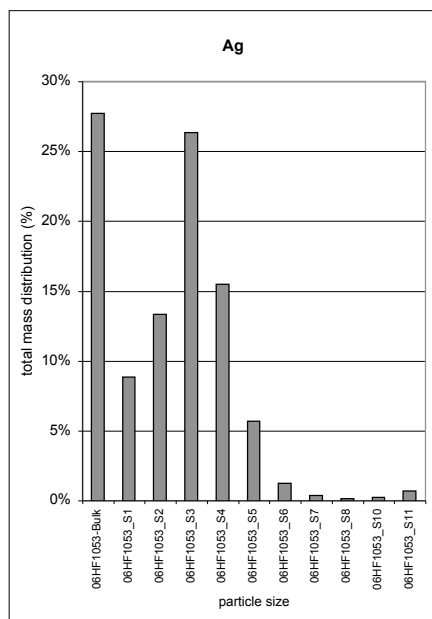
ME-MS61 U ppm	ME-MS61 V ppm	ME-MS61 W ppm	ME-MS61 Y ppm	ME-MS61 Zn ppm	ME-MS61 Zr ppm
0.6	158	0.7	16.2	62	23.6
0.8	198	1.2	26.6	63	44.9
0.6	186	0.8	23	64	31.8
0.7	161	0.9	20.4	61	34.2
0.7	129	0.7	16.4	52	28.1
0.8	146	1.1	18.8	60	30.2
0.9	197	1	25.8	73	31.6
1.4	303	1.6	41.9	101	41.6
1.5	302	2.1	40.8	110	61.4
1.3	250	2.4	34.4	131	50.5
1.4	249	2	30.9	154	58.4



S1 > 2830 um	1000 um > S4 > 500 um	125 um > S7 > 75 um	32 um > S10 > 20 um
2830 um > S2 > 1700 um	500 um > S5 > 250 um	75 um > S8 > 45 um	20 um > S11
1700 um > S3 > 1000 um	250 um > S6 > 125 um	45 um > S9 > 32 um	

Elemental Distribution (by Mass %) vs. Particle Size

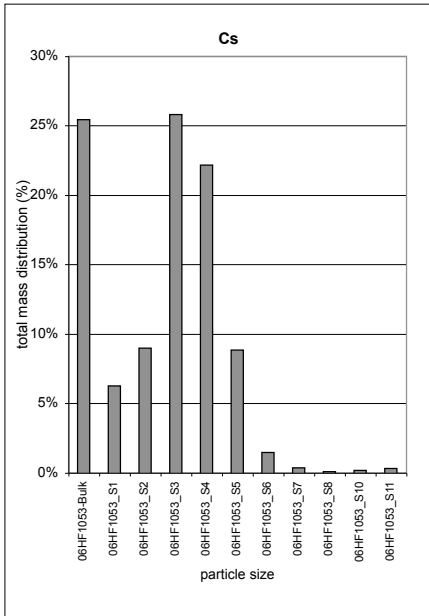
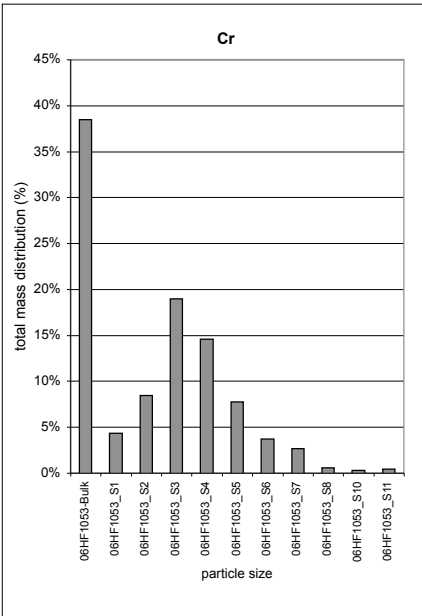
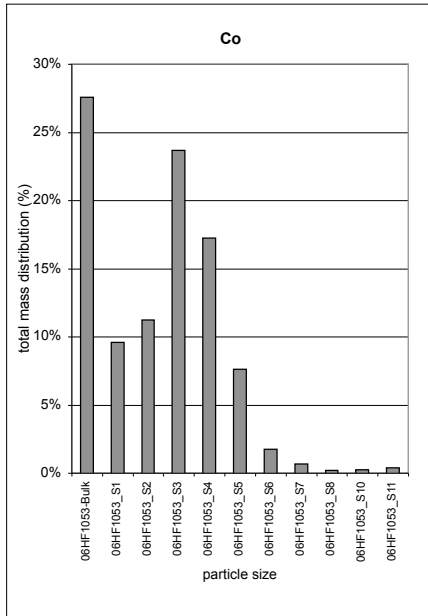
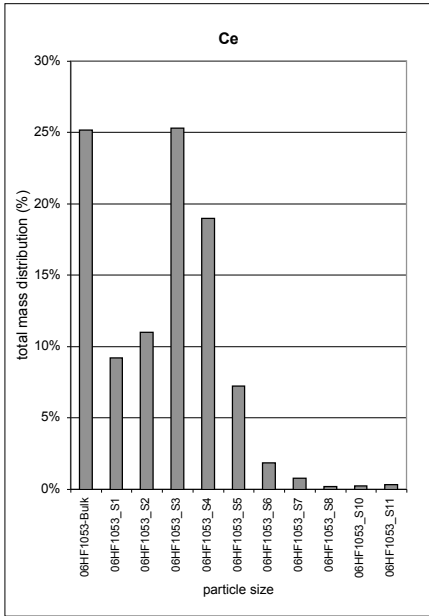
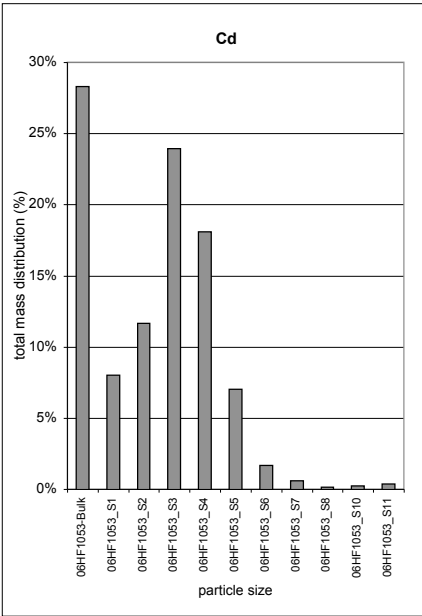
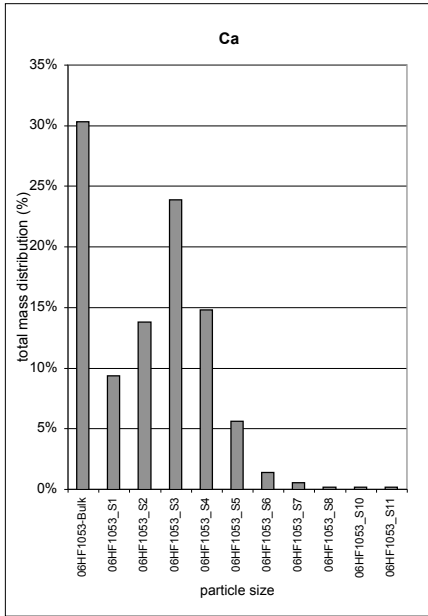
TOTAL MASS (mg)		0.34	221430.05	22.47	1424.82	2.94	0.22
SAMPLE DESCRIPTION	Recvd Wt.	Ag %	Al %	As %	Ba %	Be %	Bi %
06HF1053-Bulk	0.08	28%	30%	28%	27%	23%	32%
06HF1053_S1	0.06	9%	9%	6%	8%	10%	9%
06HF1053_S2	0.18	13%	11%	9%	10%	11%	12%
06HF1053_S3	0.06	26%	24%	26%	25%	28%	22%
06HF1053_S4	0.08	15%	18%	19%	22%	19%	17%
06HF1053_S5	0.08	6%	6%	8%	7%	7%	5%
06HF1053_S6	0.16	1%	1%	2%	1%	2%	1%
06HF1053_S7	0.04	0%	0%	1%	0%	0%	0%
06HF1053_S8	0.02	0%	0%	0%	0%	0%	0%
06HF1053_S10	0.02	0%	0%	0%	0%	0%	0%
06HF1053_S11	0.02	1%	0%	1%	0%	0%	0%



S1 > 2830 um	1000 um > S4 > 500 um	125 um > S7 > 75 um	32 um > S10 > 20 um
2830 um > S2 > 1700 um	500 um > S5 > 250 um	75 um > S8 > 45 um	20 um > S11
1700 um > S3 > 1000 um	250 um > S6 > 125 um	45 um > S9 > 32 um	

Elemental Distribution (by Mass %) vs. Particle Size

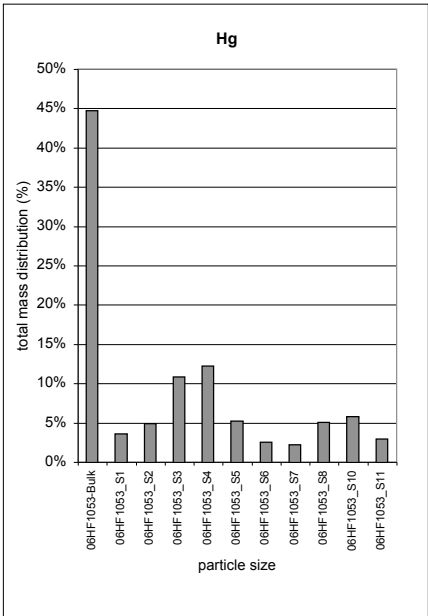
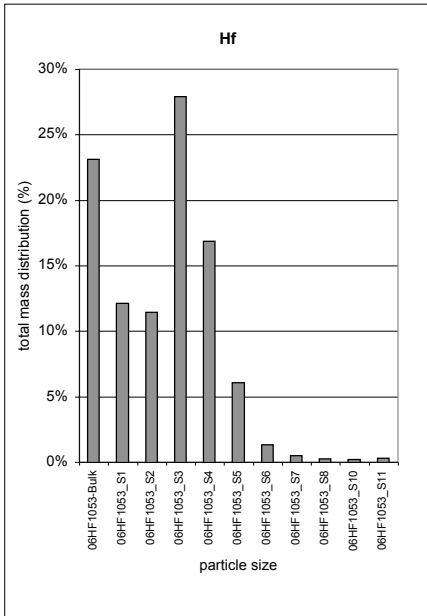
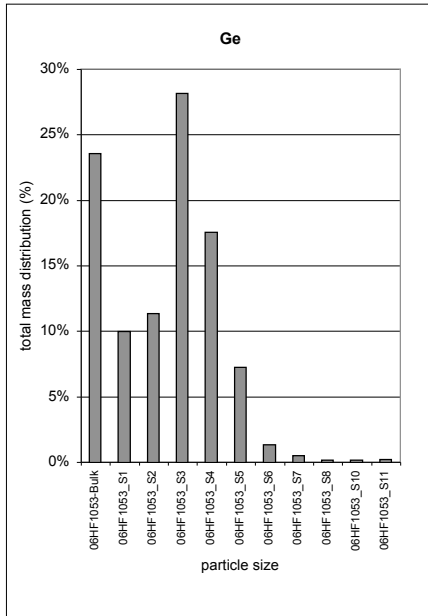
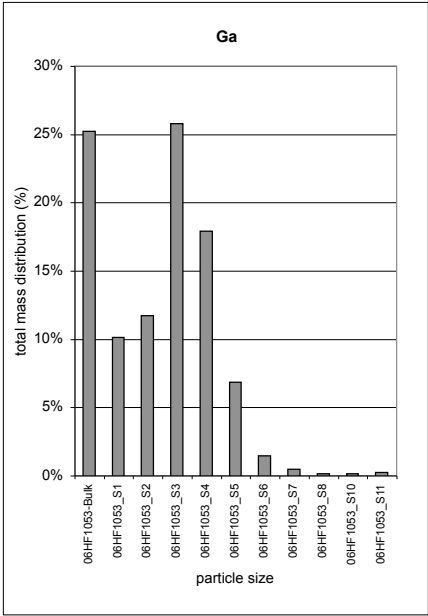
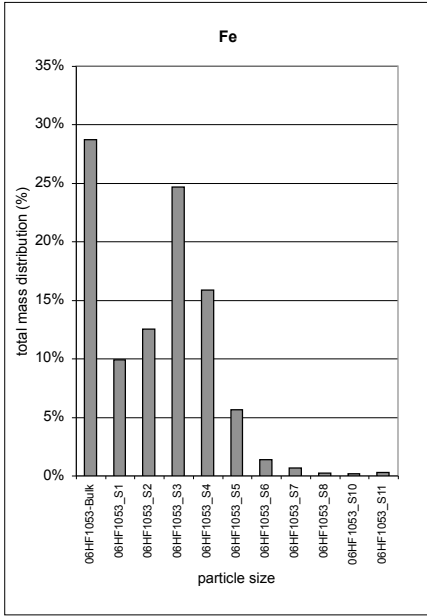
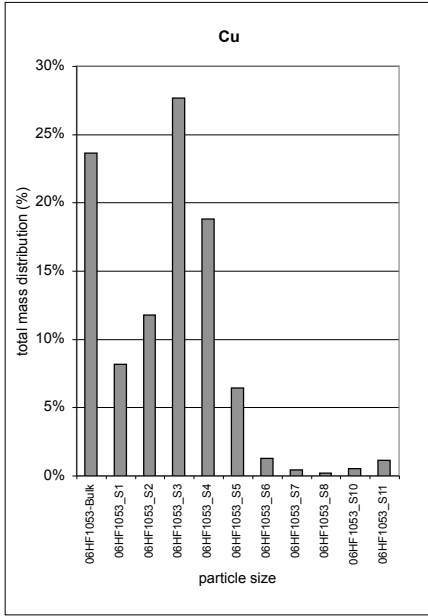
107823.18	0.57	65.16	78.03	673.13	3.88
Ca	Cd	Ce	Co	Cr	Cs
%	%	%	%	%	%
30%	28%	25%	28%	38%	25%
9%	8%	9%	10%	4%	6%
14%	12%	11%	11%	8%	9%
24%	24%	25%	24%	19%	26%
15%	18%	19%	17%	15%	22%
6%	7%	7%	8%	8%	9%
1%	2%	2%	2%	4%	1%
1%	1%	1%	1%	3%	0%
0%	0%	0%	0%	1%	0%
0%	0%	0%	0%	0%	0%
0%	0%	0%	0%	0%	0%



S1 > 2830 um	1000 um > S4 > 500 um	125 um > S7 > 75 um	32 um > S10 > 20 um
2830 um > S2 > 1700 um	500 um > S5 > 250 um	75 um > S8 > 45 um	20 um > S11
1700 um > S3 > 1000 um	250 um > S6 > 125 um	45 um > S9 > 32 um	

Elemental Distribution (by Mass %) vs. Particle Size

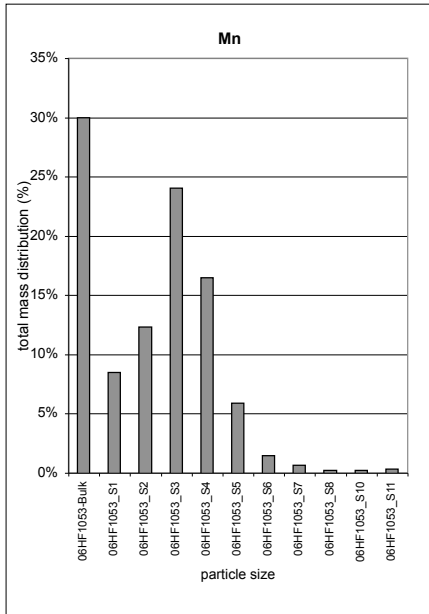
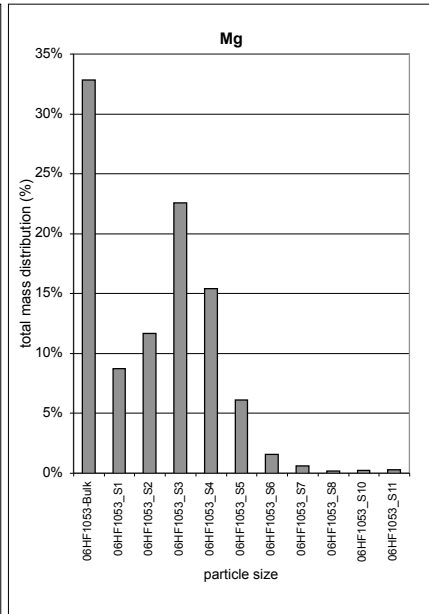
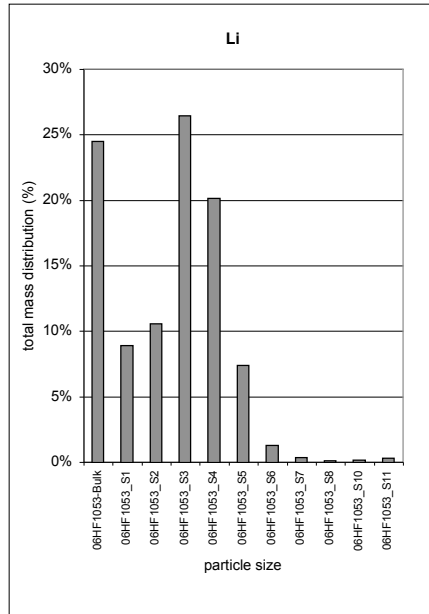
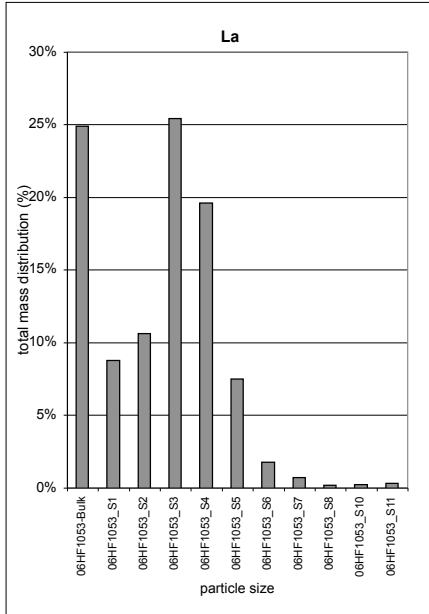
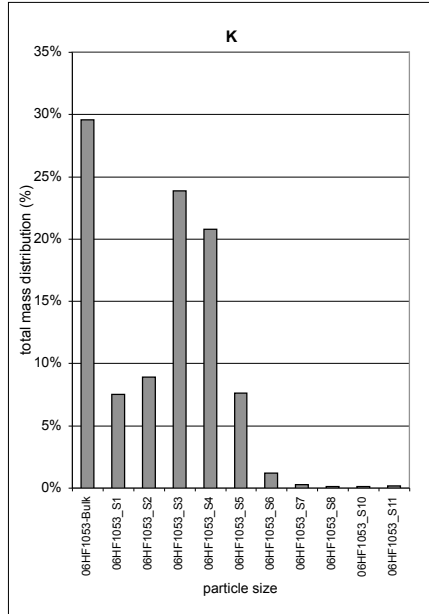
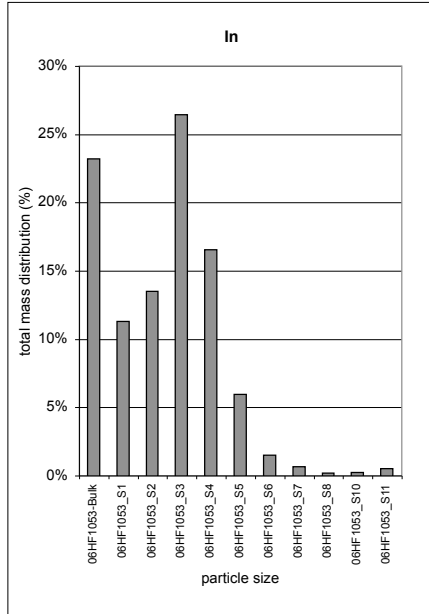
136.13	173523.39	58.04	0.59	3.52	0.18
Cu %	Fe %	Ga %	Ge %	Hf %	Hg %
24%	29%	25%	24%	23%	45%
8%	10%	10%	10%	12%	4%
12%	13%	12%	11%	11%	5%
28%	25%	26%	28%	28%	11%
19%	16%	18%	18%	17%	12%
6%	6%	7%	7%	6%	5%
1%	1%	1%	1%	1%	3%
0%	1%	0%	0%	1%	2%
0%	0%	0%	0%	0%	5%
1%	0%	0%	0%	0%	6%
1%	0%	0%	0%	0%	3%



S1 > 2830 um	1000 um > S4 > 500 um	125 um > S7 > 75 um	32 um > S10 > 20 um
2830 um > S2 > 1700 um	500 um > S5 > 250 um	75 um > S8 > 45 um	20 um > S11
1700 um > S3 > 1000 um	250 um > S6 > 125 um	45 um > S9 > 32 um	

Elemental Distribution (by Mass %) vs. Particle Size

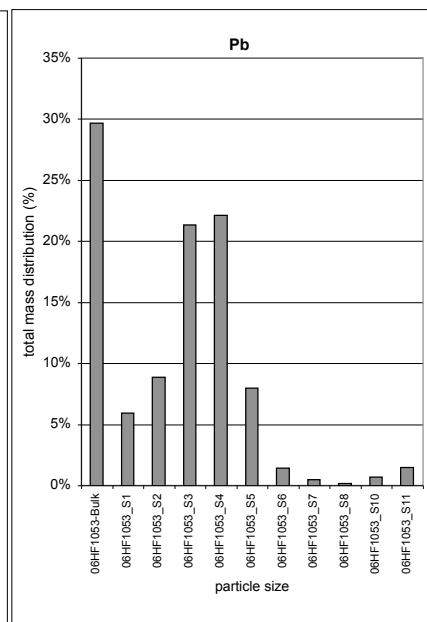
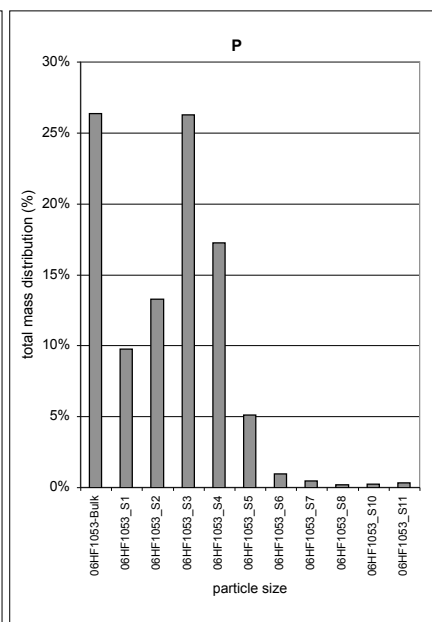
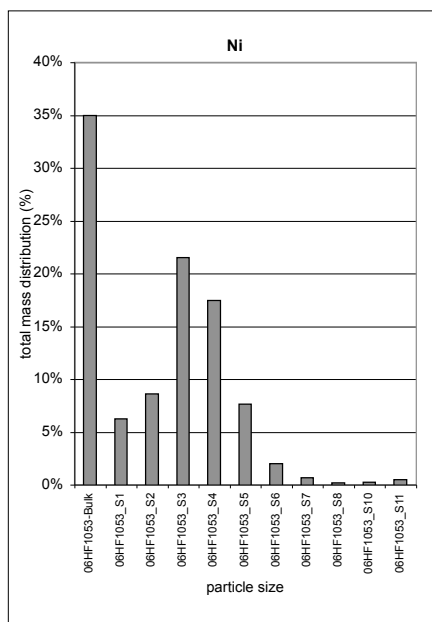
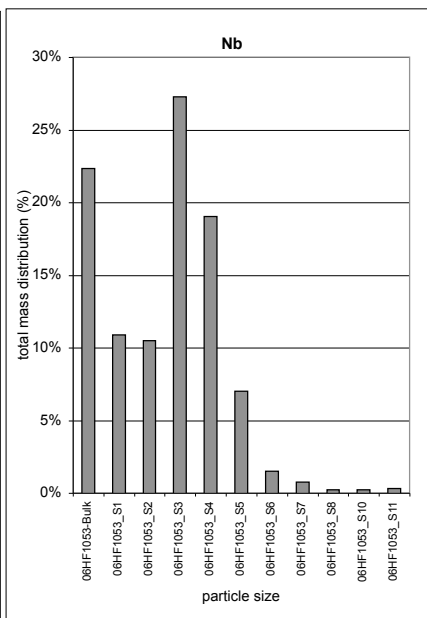
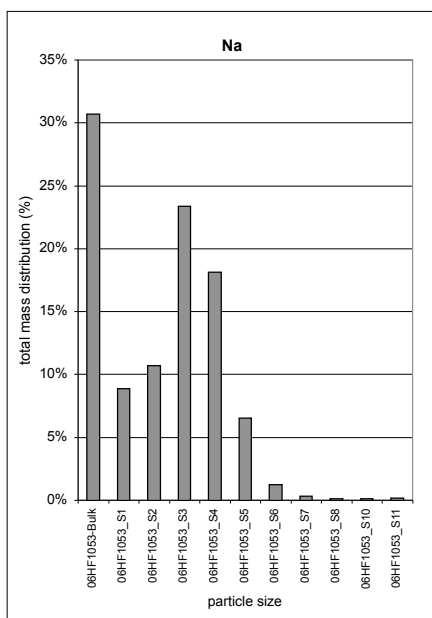
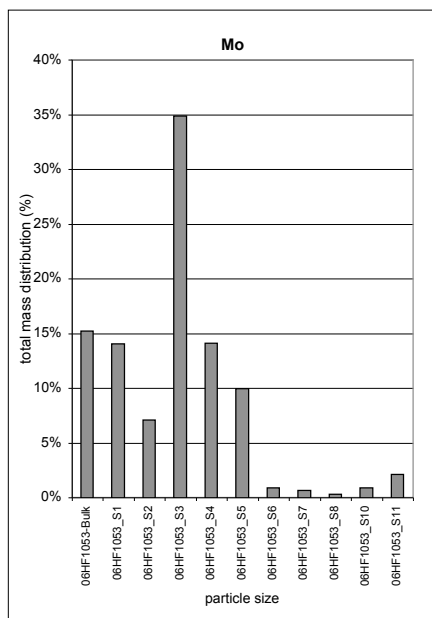
	0.22	27136.78	37.80	51.25	77499.35	3055.16
	In	K	La	Li	Mg	Mn
	%	%	%	%	%	%
	23%	30%	25%	24%	33%	30%
	11%	8%	9%	9%	9%	8%
	13%	9%	11%	11%	12%	12%
	26%	24%	25%	26%	23%	24%
	17%	21%	20%	20%	15%	16%
	6%	8%	7%	7%	6%	6%
	1%	1%	2%	1%	2%	1%
	1%	0%	1%	0%	1%	1%
	0%	0%	0%	0%	0%	0%
	0%	0%	0%	0%	0%	0%
	1%	0%	0%	0%	0%	0%



S1 > 2830 um	1000 um > S4 > 500 um	125 um > S7 > 75 um	32 um > S10 > 20 um
2830 um > S2 > 1700 um	500 um > S5 > 250 um	75 um > S8 > 45 um	20 um > S11
1700 um > S3 > 1000 um	250 um > S6 > 125 um	45 um > S9 > 32 um	

Elemental Distribution (by Mass %) vs. Particle Size

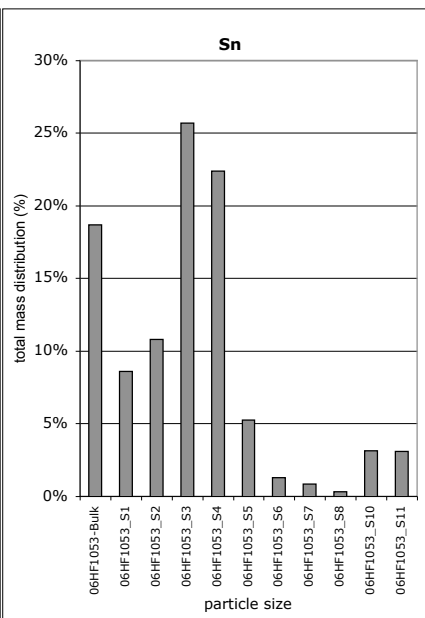
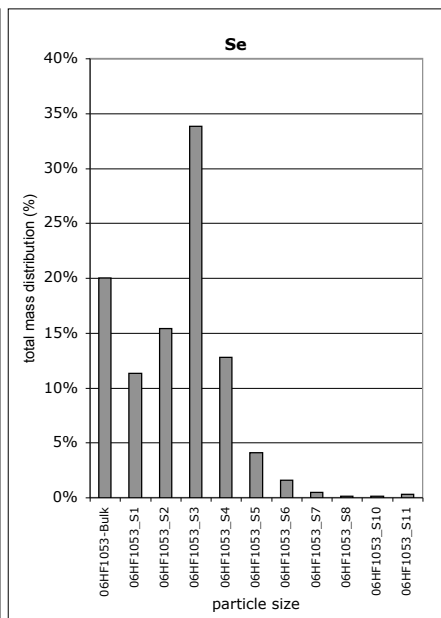
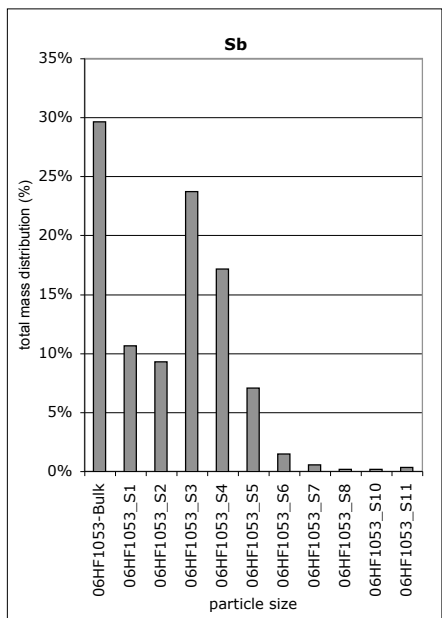
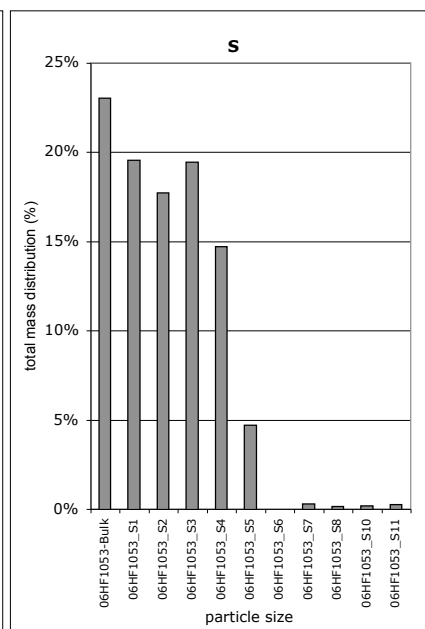
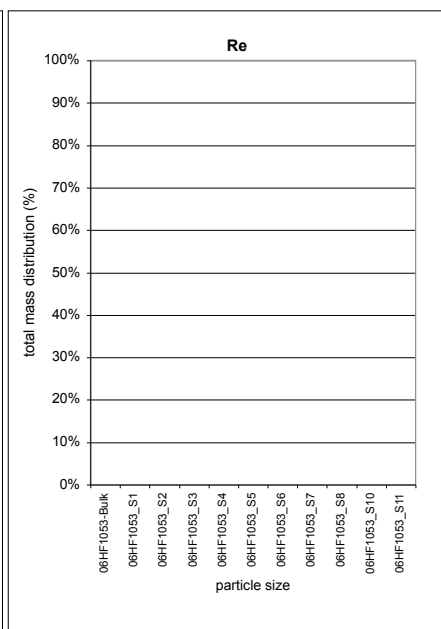
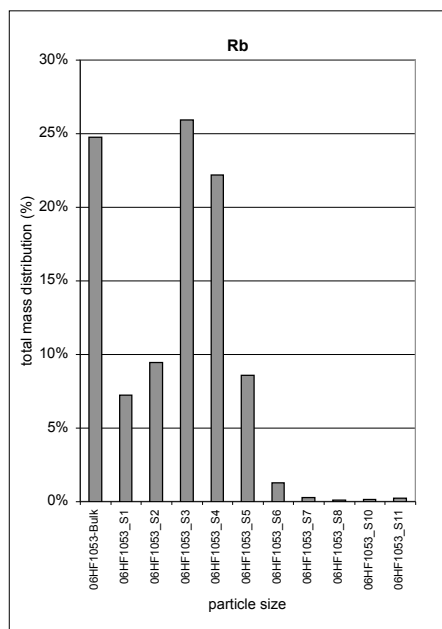
	2.90	64706.88	18.71	435.21	1720.48	21.16
	Mo	Na	Nb	Ni	P	Pb
	%	%	%	%	%	%
	15%	31%	22%	35%	26%	30%
	14%	9%	11%	6%	10%	6%
	7%	11%	11%	9%	13%	9%
	35%	23%	27%	21%	26%	21%
	14%	18%	19%	17%	17%	22%
	10%	7%	7%	8%	5%	8%
	1%	1%	2%	2%	1%	1%
	1%	0%	1%	1%	0%	0%
	0%	0%	0%	0%	0%	0%
	1%	0%	0%	0%	0%	1%
	2%	0%	0%	0%	0%	1%



S1 > 2830 um	1000 um > S4 > 500 um	125 um > S7 > 75 um	32 um > S10 > 20 um
2830 um > S2 > 1700 um	500 um > S5 > 250 um	75 um > S8 > 45 um	S11
1700 um > S3 > 1000 um	250 um > S6 > 125 um	45 um > S9 > 32 um	

Elemental Distribution (by Mass %) vs. Particle Size

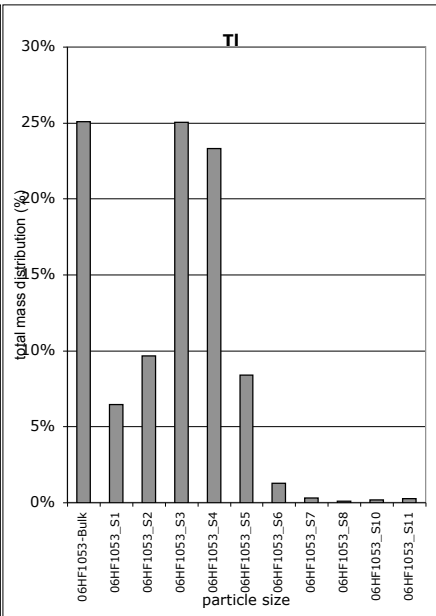
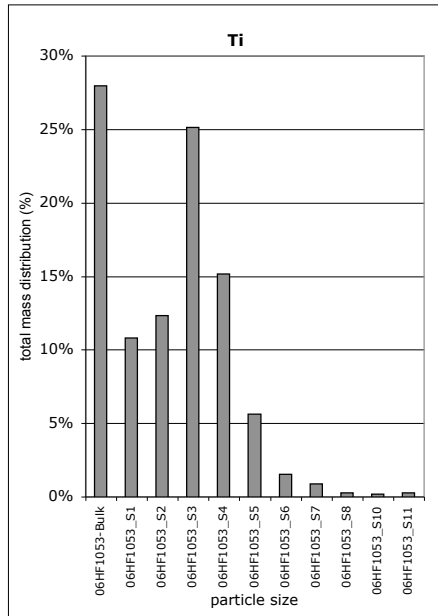
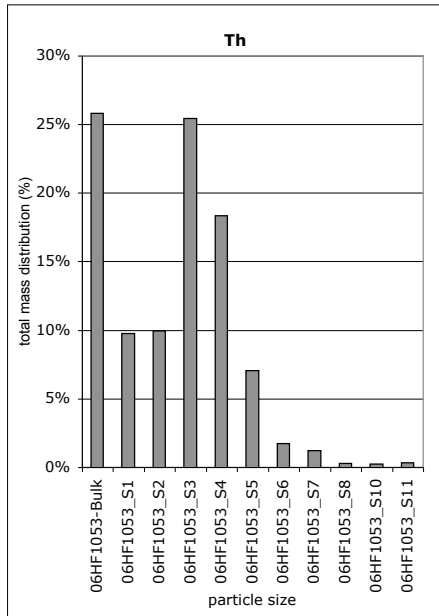
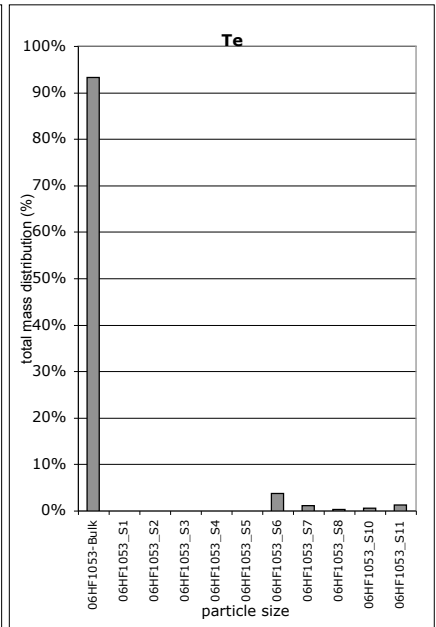
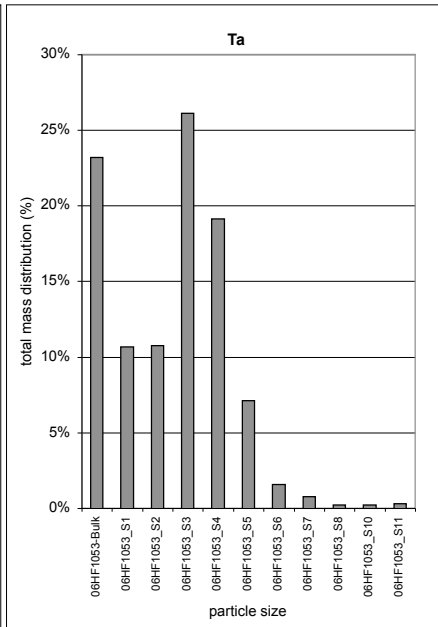
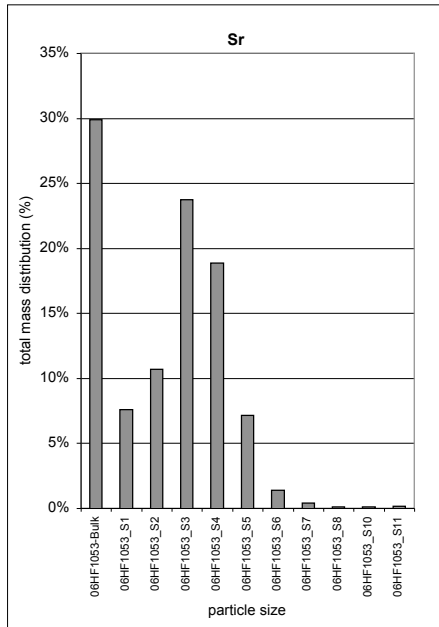
80.34	0.00	504.26	2.94	5.81	4.97
Rb	Re	S	Sb	Se	Sn
%	%	%	%	%	%
25%	0%	23%	30%	20%	19%
7%	0%	20%	11%	11%	9%
9%	0%	18%	9%	15%	11%
26%	0%	19%	24%	34%	26%
22%	0%	15%	17%	13%	22%
9%	0%	5%	7%	4%	5%
1%	0%	0%	1%	2%	1%
0%	0%	0%	1%	0%	1%
0%	0%	0%	0%	0%	0%
0%	0%	0%	0%	0%	3%
0%	0%	0%	0%	0%	3%



S1 > 2830 um	1000 um > S4 > 500 um	125 um > S7 > 75 um	32 um > S10 > 20 um
2830 um > S2 > 1700 um	500 um > S5 > 250 um	75 um > S8 > 45 um	20 um > S11
1700 um > S3 > 1000 um	250 um > S6 > 125 um	45 um > S9 > 32 um	

Elemental Distribution (by Mass %) vs. Particle Size

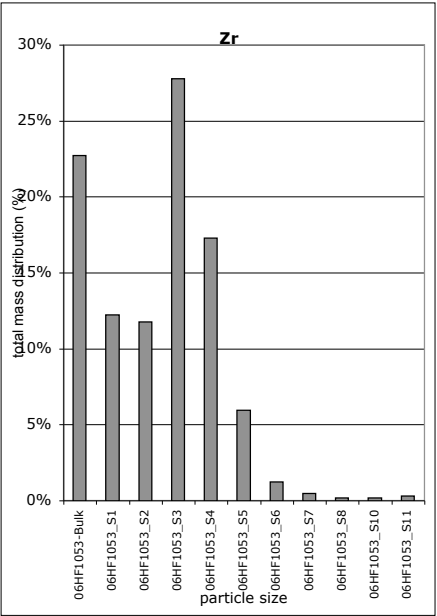
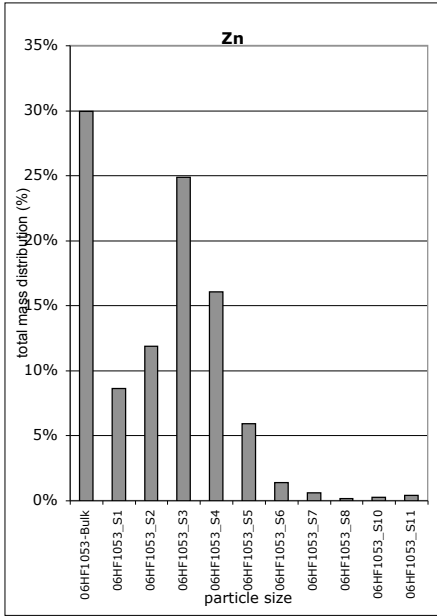
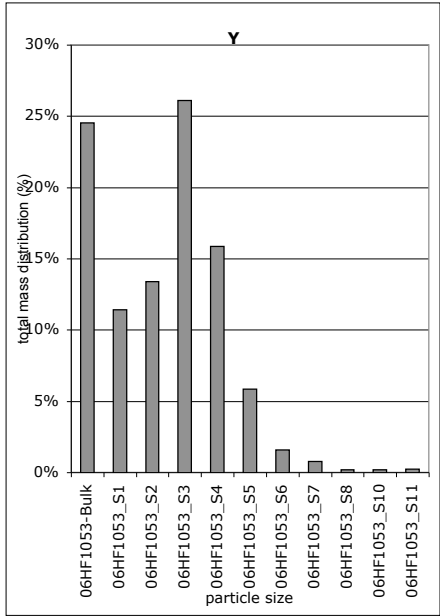
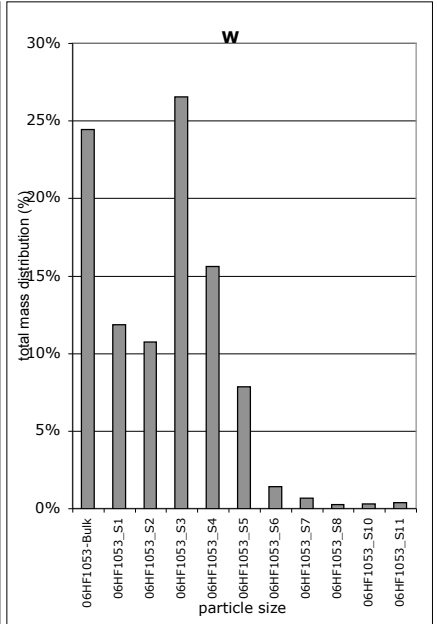
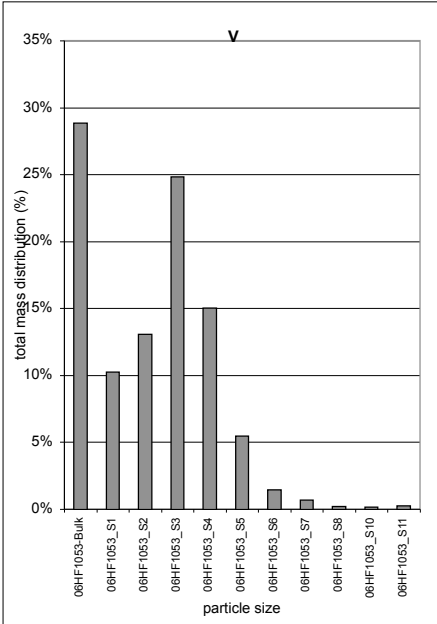
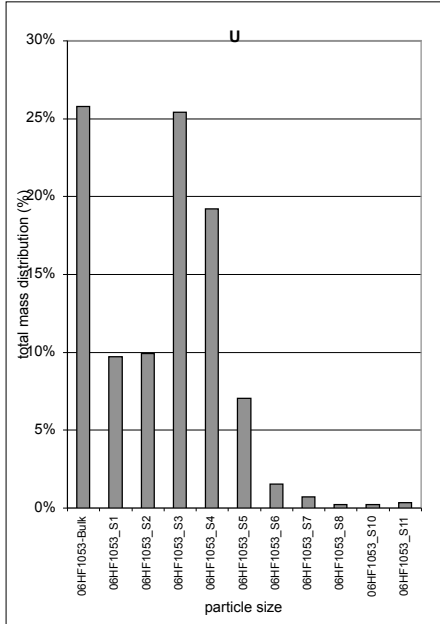
614.22		1.20		0.06		8.10		17576.40		0.51	
Sr	Ta	Te	Th	Ti	Tl	Sr	Ta	Te	Th	Ti	Tl
%	%	%	%	%	%	%	%	%	%	%	%
30%	23%	93%	26%	28%	25%	30%	23%	93%	26%	28%	25%
8%	11%	0%	10%	11%	6%	8%	11%	0%	10%	11%	6%
11%	11%	0%	10%	12%	10%	11%	11%	0%	10%	12%	10%
24%	26%	0%	25%	25%	25%	24%	26%	0%	25%	25%	25%
19%	19%	0%	18%	15%	23%	19%	19%	0%	18%	15%	23%
7%	7%	0%	7%	6%	8%	7%	7%	0%	7%	6%	8%
1%	2%	4%	2%	2%	1%	1%	2%	2%	2%	2%	1%
0%	1%	1%	1%	1%	0%	0%	1%	1%	1%	1%	0%
0%	0%	0%	0%	0%	0%	0%	0%	0%	0%	0%	0%
0%	0%	1%	0%	0%	0%	0%	0%	1%	0%	0%	0%
0%	0%	1%	0%	0%	0%	0%	0%	1%	0%	0%	0%
0%	0%	1%	0%	0%	0%	0%	0%	1%	0%	0%	0%



S1 > 2830 um	1000 um > S4 > 500 um	125 um > S7 > 75 um	32 um > S10 > 20 um
2830 um > S2 > 1700 um	500 um > S5 > 250 um	75 um > S8 > 45 um	20 um > S11
1700 um > S3 > 1000 um	250 um > S6 > 125 um	45 um > S9 > 32 um	

Elemental Distribution (by Mass %) vs. Particle Size

2.70		636.92		3.33		76.72		240.63		120.76	
U		V		W		Y		Zn		Zr	
%		%		%		%		%		%	
26%		29%		24%		25%		30%		23%	
10%		10%		12%		11%		9%		12%	
10%		13%		11%		13%		12%		12%	
25%		25%		27%		26%		25%		28%	
19%		15%		16%		16%		16%		17%	
7%		5%		8%		6%		6%		6%	
2%		1%		1%		2%		1%		1%	
1%		1%		1%		1%		1%		0%	
0%		0%		0%		0%		0%		0%	
0%		0%		0%		0%		0%		0%	
0%		0%		0%		0%		0%		0%	



S1 > 2830 um	1000 um > S4 > 500 um	125 um > S7 > 75 um	32 um > S10 > 20 um
2830 um > S2 > 1700 um	500 um > S5 > 250 um	75 um > S8 > 45 um	20 um > S11
1700 um > S3 > 1000 um	250 um > S6 > 125 um	45 um > S9 > 32 um	

